TELOMERE RESOLUTION AND GENOMIC INSTABILITY IN MOUSE EMBRYONIC STEM CELLS

by

Kathleen Lisaingo

B.Sc. (Hons), The University of British Columbia, 2004

A THESIS SUBMITTED IN PARTIAL FULFILLMENT OF
THE REQUIREMENTS FOR THE DEGREE OF

DOCTOR OF PHILOSOPHY

in

THE FACULTY OF GRADUATE STUDIES

(Experimental Medicine)

THE UNIVERSITY OF BRITISH COLUMBIA
(Vancouver)

August 2012

Abstract

Proper segregation of replicated chromosomes is essential for cell division in all organisms. Linear eukaryotic chromosomes contain specialized protective structures at the chromosome ends, called telomeres, which are essential for maintaining genome stability. Telomere associations have been observed during key cellular processes including mitosis, meiosis and carcinogenesis. These telomere associations need to be resolved prior to cell division to avoid loss of telomere function. TRF1, a core component of the telomere protein complex shelterin, has been implicated as a mediator of telomere associations. To determine the effect of TRF1 protein levels on telomere associations, we used live-cell fluorescence microscopy to visualize telomeres and chromosome dynamics in cells expressing defined levels of TRF1. Elevated levels of TRF1 induced anaphase bridges containing thin “thread-like” stretches of TRF1 foci connecting segregating chromosomes. We also observed telomere aggregates, mitotic bypass, and TRF1 bridges persisting into the following cell cycle. To examine the role of TRF1 in these telomere associations, we generated a TRF1 protein which can be inducibly cleaved by TEV protease. Telomere aggregates appeared to resolve upon cleavage of TRF1 proteins, suggesting that telomere associations result primarily from protein interactions mediated by TRF1. The essential helicase RTEL1 was observed at the extremities of persistent TRF1 bridges, possibly indicating a function for RTEL1 in the resolution of TRF1-induced telomere associations. Taken together, our results demonstrate that precise regulation of TRF1 levels is essential for telomere resolution and mitotic segregation.

Preface

All experiments in Chapters 2 and 3 were designed and performed by myself. Results from Chapters 2, 3, and Figure 16A are currently being prepared for submission of a first author publication. Results in Chapter 4, excluding Figure 16A, were a partial collaboration with Dr. Evert-Jan Uringa who created the construct for RTEL1-YFP and assisted with experimental design. All experiments in Chapter 4 were performed by myself. The majority of results from Chapter 4 have been published in a second author publication (ASCB: Mol. Biol.Cell, Uringa, Lisaingo et al. 2012) [1], excluding Figure 16A. A review has also been published in a third author publication, which includes Figure 17 (Oxford Journals: Nucleic Acids Res., Uringa et al. 2010) [2]. All other experiments were designed and conducted by myself. Mike Schertzer generated the fluorescent fusion constructs for Histone 2B, 53BP1, and the fluorescent backbone of YFP/RFP-TRF1 and $TRF1_{IRES\text{-}YFP}$. All other constructs, including constructs used for cleavable TRF1 assay were generated by myself. The following figures were reprinted with permission: Figure 2 (Elsevier: DNA Repair, Denchi et al. 2009) [3], Figure 3 (Nature Publishing Group: EMBO, Bianchi et al., 1999) [4], Figures 13-15, 16B and Movies 12-14 (ASCB: Mol. Biol.Cell, Uringa, Lisaingo et al. 2012) [1], and Figure 17 (Oxford Journals: Nucleic Acids Res., Uringa et al. 2010) [2].

Table of Contents

List of Figures

List of Movies

Acknowledgements

I would like to thank my supervisor Dr. Peter Lansdorp for allowing me to work on this exciting project, for encouraging me to explore novel techniques, and for giving me the freedom to pursue my own research interests. I am extremely grateful to Dr. Ester Falconer for her insightful comments, time-spent helping me with many aspects of my research, and for challenging me to always think and write logically. I would like to express my gratitude to my committee members Dr. Rob Kay, Dr. Geoff Wasteneys, and Dr. Shoukat Dedhar for their excellent comments, advice, and understanding. Thanks to Dr. Evert-Jan Uringa for a good collaborative effort, helpful discussions, and for the RTEL1 construct. Thanks also to Mike Schertzer for constructs (as specified in Preface). Many thanks also to Dr. Geraldine Aubert for helpful telomere discussions and comments on this manuscript. I would like to express sincere gratitude to my many colleagues, past and present, for providing an excellent support system in the lab, for surrounding me with a wealth of knowledge and a wide range of expertise, and for providing a fun working environment. Thank you to the flow cytometry staff for their assistance, and for trusting me to use the cell sorters with limited supervision.

My deepest gratitude goes to my family for their support, guidance and encouragement over the years. Above all, I would like to thank my partner Kevin Hazelwood for his unwavering love and support and to whom I dedicate this thesis. A small note of thanks also to S.

Chapter 1: Introduction

1.1 Telomeres

The genome contains all the hereditary information of a living organism. The genome of eukaryotes is organized into linear chromosomes, which must be accurately copied and segregated during each cell division. The integrity of chromosomes depends on essential protective structures called telomeres. Telomeres are composed of short tandem DNA repeats and associated proteins located at the ends of chromosomes [5]. The first studies describing telomeres were performed by Hermann Muller and Barbara McClintock in the early 1930s, who noted that the ends of chromosomes must have unique protective properties which distinguish the natural ends of linear chromosomes from broken chromosome ends. Muller used X-ray irradiation in *Drosophila* to induce chromosome aberrations and observed that broken chromosome ends fused to other broken ends producing chromosome rearrangements, whereas the natural ends of chromosomes were more stable and generally did not undergo fusion events [6]. McClintock further expanded on these studies by noting that fused chromosome ends which were not resolved prior to cell division, led to chromosome bridging in anaphase of *Zea mays* [7]. She concluded that the bridges were caused by the poleward segregation of dicentric chromosomes, where the force generated by movement of the two centromeres to either pole, led to chromosome breaks at variable positions. These chromatin breaks were observed to continue to fuse and break in subsequent cell cycles, giving rise to breakage-fusion-bridge cycles, which contribute to genomic instability. Many studies since then have shown that telomeres protect chromosome ends from being recognized as DNA double-strand breaks, thus preventing activation of

the DNA damage response, chromosome end fusions, chromosome degradation by exonucleases, and aberrant repair or recombination events (reviewed in [8]). Therefore, telomeres are essential for maintaining genomic stability.

1.2 Telomere length regulation

Telomeres shorten with each cell division. Several mechanisms have been described to explain telomere shortening. The first mechanism proposes that the DNA replication machinery is unable to fully copy the ends of telomeric DNA, termed the “end-replication problem” [9, 10]. DNA replication is unidirectional, and requires an existing primer to initiate DNA synthesis. During lagging strand synthesis of the 3' strand of telomeres, RNA primers initiate synthesis of short Okazaki fragments. Following removal of the most distal RNA primer, there remains a gap at the chromosome end which cannot be filled in by DNA polymerase. This gives rise to a 3’ single strand DNA (ssDNA) overhang following replication of the lagging strand. However, this presents an apparent paradox [11]. Leading strand synthesis is continuous and should theoretically proceed to the terminus of the chromosome, giving rise to a blunt end. However both ends of the chromosome contain a 3’ ssDNA overhang of about 50-100 bases in humans and mice [12, 13], and telomere shortening by the end-replication problem only accounts for a small proportion (8-12 bases) of the total telomere loss (50-200 bases) observed with each cell cycle in most human somatic cells [14, 15]. Therefore, a second mechanism for telomere loss has been proposed which suggests that telomeres undergo end processing by resection of the 5’ strand by a sequence specific helicase or nuclease, consistent with the finding that the 5’ end of human telomeres generally ends

in the sequence ATC-5' [11, 16-18]. However, it remains unclear how end-processing is mediated or what proteins might be involved. Other proposed mechanisms for telomere loss suggest that telomere loss does not occur at every replication cycle but instead occurs sporadically. For example, oxidative DNA damage has been shown to accelerate telomere shortening during aging by inducing DNA damage preferentially at guanine-rich telomeric DNA [19, 20]. Furthermore, unresolved or improperly processed higher-order structures which have been proposed to form at guanine-rich DNA during lagging strand replication can lead to deletion of telomeres (reviewed in [21]).

When telomeres become critically short, they lose their protective function and can activate a DNA damage response, resulting in senescence or programmed cell death (apoptosis) [22]. Telomere shortening can be overcome by activation of the reverse transcriptase telomerase, which can add telomere repeats onto the 3' end of pre-existing telomeres using an intrinsic RNA molecule as a template [23, 24].

1.3 Telomeres and aging

Most human somatic cells do not have sufficient telomerase activity to maintain telomere length (about 2 to 15 kb), and undergo telomere shortening with each cell cycle [25, 26]. In contrast, laboratory mice (*Mus musculus*) have higher levels of telomerase activity and longer telomeres (about 40 to 150 kb) [27, 28]. Although telomere length is relatively stable in these mice at a younger age, older mice (of 2 years) exhibit a rapid decline in telomere length [29], suggesting that the increased telomerase activity in mice is not sufficient to maintain telomere length indefinitely.

Rapidly proliferating cells such as germ cells, and embryonic stem cells upregulate telomerase and telomere length is maintained over repeated cell divisions. In comparison, in most adult human stem cells, telomerase activity is low to undetectable and is upregulated upon rapid cellular expansion, for example in committed progenitor cells (reviewed in [30, 31]). However re-expression of telomerase in adult stem cells is not sufficient to maintain telomere length.

The gradual loss of telomere repeats with each cell division in somatic cells has been proposed to act as a tumour suppressor mechanism by limiting the maximum number of times a cell can divide, thus preventing excessive clonal expansion (reviewed in [30]). When cells eventually reach this proliferative limit, they enter cellular senescence or undergo apoptosis.

1.4 Telomeres and cancer

Tumor cells can overcome senescence and continue to divide by inactivating cell cycle checkpoint pathways, such as the p53 checkpoint, however telomeres continue to shorten with each cell division and this is not sufficient to immortalize them. As these cells continue to divide they eventually enter a state of crisis where cells in the population exhibit severe genomic instability and the majority of cells undergo apoptosis [32]. This drives the selection of rare cells from the population that can re-express telomerase. These cells are considered to be immortal since they can divide indefinitely under defined culture conditions while maintaining telomere length and without entering

senescence or crisis. Telomerase activation has been found in the majority (~90%) of human tumors and is believed to be a key step in tumorigenesis (reviewed in [33]). A small proportion of human tumors appear to maintain telomere length in the absence of telomerase by using an alternative recombination-based mechanism. These cells are characterized by highly heterogeneous telomere lengths, which appear to be mediated by homologous recombination between telomeres (reviewed in [34]).

1.5 Telomere structure

The unique structure of telomeres provides stability and protection for the chromosome end. Telomeric DNA is composed of tandem arrays of guanine-rich repeats for most of its length, with a 3' ssDNA overhang at the extreme end. Telomeric DNA in vertebrates is composed of the sequence $(5'\text{-TTAGGG-}3')_n$. Electron microscopy studies have shown that the telomere can form a "lariat" structure known as a T loop where the telomere folds back on itself, by invasion of the 3' ssDNA overhang into duplex telomeric DNA (Figure 1) [35, 36]. At the base of the T loop, a second loop is formed by the strand displaced by invasion of the 3' ssDNA overhang, termed the displacement loop (D loop) (Figure 1). T loops have been observed in telomeric DNA from a range of organisms, including humans and mice [35, 36]. The size of T loops appears to be variable within individual telomeres from a single cell, as well as between species, suggesting that size is not a constraint on T loop function. By effectively hiding the chromosome end, the T loop is thought to shield telomeres from detection by the DNA repair machinery, as well as regulate access of telomerase to the telomere (reviewed in [37, 38]). However, the dynamics of T loop formation and resolution are not

well characterized. It is not clear whether T loops form during certain stages of the cell cycle or whether they are resolved during telomere processing events, such as during telomere replication or repair. Furthermore, it is unclear whether certain factors, such as helicases, might be recruited to telomeres to resolve T loops.

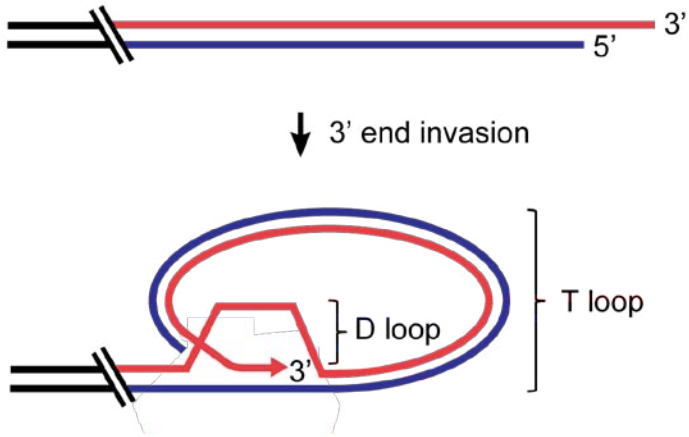

Figure 1. Telomeres form a T loop structure.

The telomere can fold back to form a T loop (telomere loop) by invasion of the 3’ ssDNA overhang into duplex telomeric DNA. At the base of the T loop, the displaced strand forms the D loop (displacement loop).

1.6 Telomere proteins

Telomeres associate with a core complex of six proteins known as shelterin (Figure 2) (reviewed in [39]). The T loop and the shelterin complex likely function together to protect telomeres by distinguishing telomeres from DNA breaks, protecting telomeres from inappropriate DNA damage responses, and regulating telomere extension by telomerase. Each of the shelterin proteins localize specifically to telomeres

during the cell cycle. Two of these proteins, TRF1 (Telomeric repeat-binding factor 1) and TRF2 (Telomeric repeat-binding factor 2), bind duplex telomeric DNA and serve to recruit and stabilize the other shelterin proteins [40-44]. Although TRF1 and TRF2 do not interact, they are linked by TIN2 (TRF1-interacting nuclear factor 2) [45]. TIN2 acts as the central linchpin of the shelterin proteins, not only binding TRF1 and TRF2, but also TPP1 [45-47]. The C-terminus of TIN2 binds the dimerization domain of TRF1, and the N-terminus of TIN2 binds the linker domain in TRF2 [48]. TPP1 stabilizes the TRF1-TIN2-TRF2 interaction [49], and recruits the shelterin protein POT1 (Protection of telomeres 1) to telomeres [50, 51]. POT1 binds the 3' ssDNA overhang of telomeres, and protects the telomere from being detected as DNA damage [52]. The final shelterin protein RAP1, binds TRF2. Although the function of RAP1 is not well characterized, loss of RAP1 leads to increased telomere recombination, suggesting a role for RAP1 in repressing telomere recombination [53]. Telomeres also associate with a number of proteins outside of the shelterin complex, however unlike the shelterin proteins, they localize and have additional functions outside of the telomere.

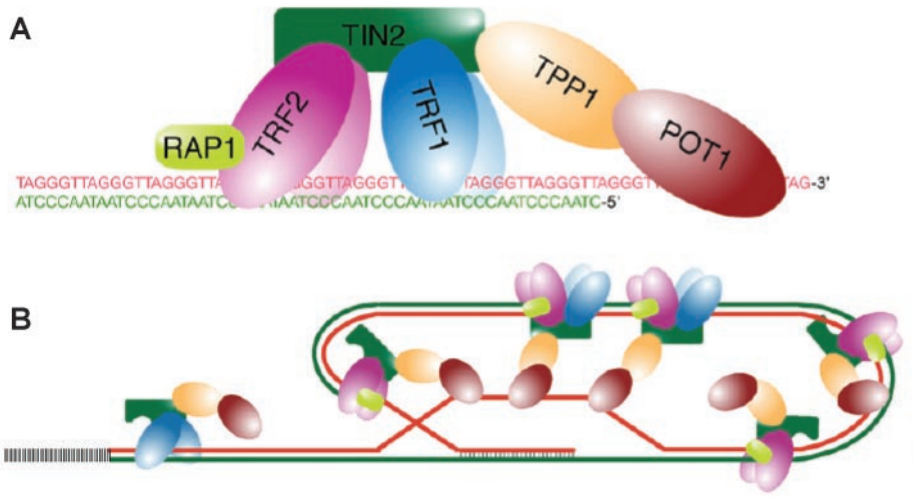

Figure 2. The shelterin complex protects telomeres.

The shelterin complex associates with the telomere and is composed of six proteins, including TRF1, TRF2, TIN2, TPP1, POT1, and RAP1 (Reprinted with permission of Elsevier: DNA Repair, Denchi et al. 2009 [3]).

1.7 TRF1

1.7.1 TRF1 structure

TRF1 protein structural domains include a dimerization domain and a Myb DNA-binding domain connected by an unstructured flexible linker, as well as a short N-terminal acidic domain (Figure 3) [4, 40, 42, 54]. The sequence identity of the dimerization domain and Myb DNA-binding domain are highly conserved (83% and 84%, respectively), whereas the flexible linker is poorly conserved (38%) between mice and humans [54]. The flexible linker is thought to impart a high degree of spatial flexibility to TRF1 [4] [55]. Electron microscopy studies demonstrated that TRF1 protein

can bind telomeric DNA probes containing Myb DNA-binding sites with variable spacing and in different orientations. In particular, when available binding sites were limited to two Myb DNA-binding sites placed far apart on the same DNA tract, TRF1 induced looping of the DNA tract, where the size of the loop corresponded to the distance between the binding sites [4]. Of note, TRF1 protein consistent with the size of a single TRF1 dimer was observed at the loop junction. Based on these studies, a model was proposed for TRF1 binding where the two DNA-binding Myb domains can recognize telomere binding sites independently, in both orientations, and at both adjacent and distant sites (Figure 3) [4].

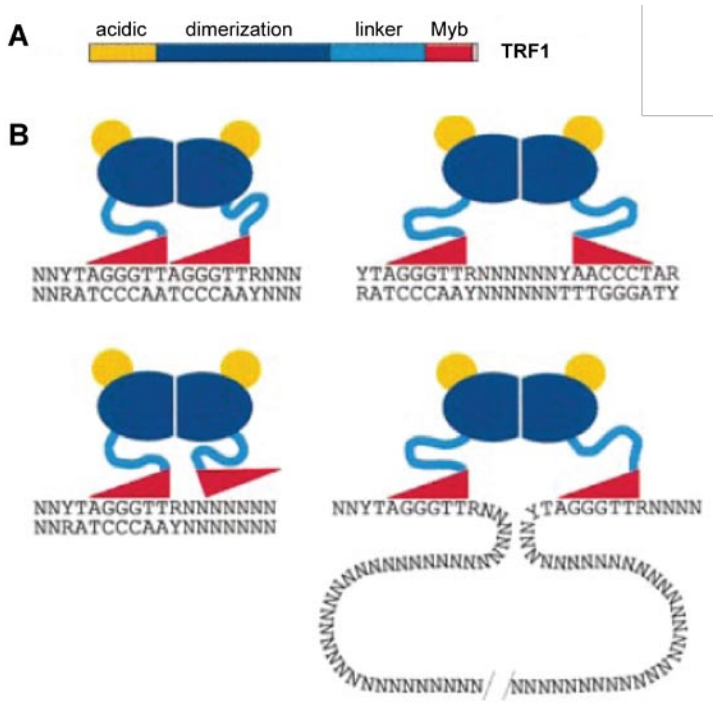

Figure 3. Model for TRF1 binding to telomeres

(A) TRF1 protein structural domains. (B) Proposed mode of TRF1 binding to telomeres showing TRF1flexibility and variable binding of Myb DNA-binding domains

(Reprinted with permission of Nature Publishing Group: EMBO, Bianchi et al., 1999 [4]).

1.7.2 Traditional function of TRF1 at telomeres

TRF1 is expressed ubiquitously, and localizes to telomeres for the duration of the cell cycle [41, 56]. Early studies have shown that TRF1 acts as a negative regulator of telomere length. Long-term overexpression of TRF1 led to gradual telomere shortening, while expression of a dominant-negative mutant, that inhibits TRF1 binding, led to telomere elongation [57]. Although TRF1 does not bind or detectably alter telomerase expression, TRF1 has been proposed to regulate telomere length by indirectly inhibiting telomerase access to the telomere 3' end [57]. Deletion of TRF1 is lethal during mouse embryonic development [58], but no evidence of impaired telomere structure or length, or deregulated telomerase activity was observed. This suggests that TRF1 has an essential function that is separate from its role in regulating telomere length.

1.7.3 Comparison of TRF1 and TRF2 structure and function

TRF1 and TRF2 have similar structural features, they both form homodimers but not heterodimers via a number of hydrophobic interactions along the interface of an internal dimerization domain [59], and each dimer binds telomeric DNA via two (one per monomer) C-terminal Myb DNA-binding domains. The dimerization and Myb domains of human TRF1 and TRF2 share a 27% and 56% sequence identity, respectively. Both TRF1 and TRF2 bind the same sequence (5'-TAGGGTT-3') of duplex telomeric DNA [60]. Whereas TRF1 has an N-terminal acidic domain [54], TRF2 has a N-terminal basic

domain. TRF2 also contains an unstructured linker, which likely has similar flexible properties to the TRF1 linker [60].

Both TRFs have been observed to induce looping of different telomeric DNA structures using electron microscopy studies. TRF1 can induce looping between duplex strands of telomeric DNA under conditions when binding sites are limited, with TRF1 protein observed specifically at the loop junction (Figure 3, right) [4]. In comparison, TRF2 promotes the transition from linear telomeric DNA to T loop formation [35]. TRF2 protein (but not TRF1 protein) was observed specifically at the base of the T loop where the 3' ssDNA overhang invades duplex telomeric DNA [35, 61]. Taken together, this suggests that TRF1 and TRF2 mediate looping of different structures at telomeres by recognizing the loop junction. However, the mechanisms by which TRF1 and TRF2 induce looping of these different telomeric DNA structures remain unclear.

Similar to TRF1, TRF2 appears to negatively regulate telomere length [62]. However, the predominant role of TRF2 appears to be protecting the telomere from being recognized as a DNA break, possibly by promoting formation of T loops [35]. Overexpression of dominant-negative TRF2 induced activation of the DNA damage response and chromosome end fusions [63, 64]. This suggests that although TRF1 and TRF2 are structurally similar, they have comparable but distinct functions at the telomere.

1.7.4 TRF1 regulation

TRF1 protein levels appear to increase in mitosis and decrease in G1 and S-phase [65, 66]. Endogenous TRF1 protein levels increased by ~1.6-fold in mitosis compared to S-phase synchronized human cells, whereas exogenously expressed (Myc-tagged) TRF1 proteins increased by ~4.3-fold [66]. Since a mitotic increase in TRF1 protein levels was observed for both endogenous and exogenous TRF1 protein, this suggests that TRF1 levels are regulated by a post-transcriptional mechanism. It is not clear why the mitosis-specific fold increase in TRF1 protein levels was greater in cells expressing exogenous TRF1 compared to endogenous TRF1 alone, however this may be a reflection of TRF1 regulation in the presence of elevated levels of TRF1. TRF1 association with telomeric chromatin was also found to increase in mitosis and decrease as cells exit mitosis in *Xenopus* cell extracts *in vitro* [67]. This suggests that both TRF1 levels and TRF1 binding to telomeres is highly regulated during the cell cycle, specifically during mitosis.

A number of mechanisms have been described that regulate TRF1 binding to and removal from telomeres. TRF1 binding to telomeres is highly dynamic (with a residence time of ~44s) [68]. TRF1 binding to telomeres is promoted by GNL3L (guanine nucleotide-binding protein-like 3) which induces TRF1 dimerization and stabilization [66]. The function of GNL3L appears to be opposed by nucleostemin, which prevents dimerization of non-telomere bound TRF1 and decreases the dynamic binding of TRF1 to telomeres [69]. Telomere-bound TRF1 is stabilized by TIN2 which prevents TRF1 poly(ADP-ribosyl)ation and subsequent dissociation and degradation of TRF1 by the

proteosome [70, 71]. TRF1 dissociation from telomeres is induced by post-translational modifications, including poly(ADP-ribosyl)ation by human tankyrase 1 and by phosphorylation by ATM [71, 72]. Pin1 is a prolyl isomerase that induces changes in protein conformation upon binding and phosphorylation of Ser/Thr-Pro motifs (reviewed in [73]). Pin1 was found to bind TRF1 at a specific Ser/Thr-Pro motif during mitosis, and depletion of Pin1 led to increased TRF1 binding to telomeres and suppression of TRF1 degradation. This suggests that Pin1 may regulate TRF1 by catalyzing a conformational change in TRF1 protein, specifically during mitosis [74]. Once removed from telomeres, unbound TRF1 is unstable, and is ubiquitinylated by Fbx4 (F-box protein) and targeted for degradation by the proteosome [75, 76]. Of note, different mechanisms for the regulation of TRF1 levels during the cell cycle may exist in humans and mice. Human tankyrase 1 binds the acidic domain of TRF1 and poly(ADP)ribosylates TRF1. However, in mice TRF1 appears to lack the tankyrase 1-binding motif and mouse tankyrase 1 does not bind or poly(ADP-ribosyl)ate TRF1 [77]. There clearly exist a number of mechanisms for careful control of TRF1 binding, removal and degradation, suggesting that precise regulation of TRF1 protein levels is important for its function at telomeres.

1.8 Role of TRF1 in telomere associations

Although the traditional role for TRF1 has involved telomere length regulation, studies have begun to reveal additional functions for TRF1. Indeed, several lines of evidence have begun to uncover a novel role for TRF1 in mediating physical interactions between telomeres. Two main classes of telomere associations have been

described: associations between the telomeres of sister chromatids, and telomere aggregates between the telomeres from different chromosomes.

Sister telomere associations have been observed during mitosis upon depletion of a TRF1 regulator. In human cells, tankyrase 1 poly(ADP-ribosyl)ates TRF1, inhibiting its binding to telomeric DNA [71]. Overexpression of tankyrase 1 leads to TRF1 dissociation from telomeres and its subsequent degradation [75], while tankyrase 1 depletion and TRF1 overexpression lead to mitotic arrest [65, 78, 79]. Tankyrase 1-depleted cells were able to enter mitosis and align their chromosomes at the metaphase plate as expected. A striking phenotype was observed at the metaphase-to-anaphase transition, where sister telomeres were unable to separate. In contrast, the centromeres and arms of sister chromatids appeared separated. This suggests that sister chromatids began to segregate poleward by separating at the centromeres and along chromosome arms, but were unable to progress past early anaphase due to associated sister telomeres [78]. These telomere associations were resolved upon depletion of TRF1 and TIN2, suggesting that TRF1 and TIN2 are required for the sister telomere associations observed during mitosis in tankyrase 1-depleted cells [80].

A second class of telomere associations involves clustering of telomeres from different chromosomes, also known as telomere aggregates. Telomere aggregates have been observed under both physiological and pathological conditions. In meiosis of diverse eukaryotes, telomeres cluster to one side of the nucleus with the chromosomes in a bouquet arrangement. This telomere meiotic bouquet is proposed to facilitate the

alignment of homologous chromosomes prior to their recombination and segregation. Studies have shown that Taz1 (the TRF1/TRF2 ortholog in *S.pombe*) is required to stabilize telomere associations during this process [81]. Although telomeres in normal human cells are distributed throughout the nucleus and for the most part do not overlap, large telomere aggregates have been observed in interphase nuclei of human tumour cells [82-85]. Taken together, these studies implicate a role for TRF1 in telomere associations occurring during mitosis, meiosis and carcinogenesis.

In vitro studies have shown that TRF1 protein alone can induce parallel pairing, and clustering of telomeric DNA tracts [55, 86]. Of note, this was observed specifically at high TRF1 concentrations, but not at low TRF1 concentrations [55]. These studies revealed that telomere associations can be induced by TRF1 alone and are favoured in the presence of elevated TRF1 protein levels.

1.9 Telomere cohesion mechanism

A mechanism has been proposed whereby telomere-specific proteins might mediate cohesion between sister telomeres [78, 87]. This telomere cohesion mechanism was based on evidence from studies showing that sister telomeres remain associated in early anaphase of tankyrase 1-depleted cells, apparently mediated by a protein interaction [78]. Since TRF1 is a target for tankyrase 1 poly(ADP)ribosylation, TRF1 was suggested to be a potential candidate for mediating telomere cohesion. However, TRF1 is only one of many potential tankyrase 1 targets, and the details of how telomere cohesion is mediated remain unclear.

Telomere cohesion by telomere-associated proteins could function to physically link sister telomeres together from replication until mitosis, in a similar manner to multi-subunit protein complexes called cohesins which link together sister chromatids at centromeres and along chromosome arms. Upon DNA replication, cohesins are thought to form a ring structure encircling the DNA strands from both sister-chromatids. Cohesin regulates chromosome segregation by dissociating from sister-chromatids in two steps. In early prophase, cohesin is removed from sister chromatid arms but a small amount of cohesin remains at centromeres. These remaining cohesins are removed at anaphase-onset by cleavage of a cohesin subunit by separase, which is thought to open the cohesin ring, leading to the segregation of sister-chromatids.

1.10 RTEL1

The helicase RTEL1 (Regulator of telomere length 1) has functions in telomere maintenance and DNA repair. RTEL1 was initially identified in genomic mapping studies as a dominant genetic factor responsible for regulating telomere length differences between strains of mice with long (*Mus musculus*) and short (*Mus spretus*) telomeres [28, 88]. RTEL1-deficient cells exhibit telomere shortening, impaired cell growth, and chromosome breaks and fusions (Ding et al., 2004). RTEL1 has also been shown to suppress homologous recombination during DNA repair [89]. Deletion of RTEL1 is lethal during mouse embryonic development, suggesting an essential function for RTEL1 [28]. Variants in the RTEL1 locus have been associated with glioma susceptibility [90-92].

Taken together, this suggests that RTEL1 is essential for telomere maintenance and genomic stability.

Telomeres were recently found to resemble specific chromosome regions which are especially prone to DNA breakage, and are generally rich in repetitive sequences, termed fragile sites ([93]). Fragile-telomere phenotypes such as multiple or elongated telomere signals indicative of DNA breakage or lack of DNA condensation were observed in mouse embryo fibroblasts in the presence of low levels of aphidicolin-induced replication stress [93]. TRF1 has been reported to suppress telomere fragility and promote replication of telomeres [93, 94]. This fragility was suppressed by RTEL1 [93], suggesting an epistatic interaction between these two genes, in which RTEL1 and TRF1 function in the same pathway to suppress telomere fragility. Based on these studies, RTEL1 was proposed to be recruited to telomeres by TRF1, possibly to resolve higher-order structures that can form at guanine-rich telomeric DNA, such as D loops and G-quadruplex DNA [28, 89, 93, 95]. G-quadruplex DNA has been shown to form a highly stable four stranded G-rich structure *in vitro* and has been proposed to form during lagging strand replication, however, the existence of G-quadruplex DNA *in vivo* remains to be determined. RTEL1 has been shown to dissociate D loop structures *in vitro* and recent evidence suggests that RTEL1 can also disassemble G-quadruplex DNA at telomeres [95].

1.11 Telomeric DNA probes

Specific labelling of telomeric DNA in the laboratory can be used to measure telomere length or to analyze telomere distribution. Peptide nucleic acids (PNA) are synthetic DNA analogs which can hybridize to complementary DNA or RNA sequences with high affinity. Since PNA does not contain negatively charged phosphase groups, there is less electrostatic repulsion with negatively charged DNA, and PNA-DNA interactions are stronger than DNA-DNA or DNA-RNA interactions. Telomere-specific PNA probes can be conjugated to fluorophores and hybridized to telomere repeats for specific labelling of telomeric DNA, known as telomere fluorescence in situ hybridization (telomere-FISH).

Several techniques to measure telomere length have been developed which exploit the use of telomere-specific probes (reviewed in [96]). Initial methods developed to measure telomere length involved labelling telomeres with radioactive telomere DNA probes, following digestion of whole genomic DNA with restriction enzymes which do not digest telomeric DNA and electrophoresis-separation of the DNA fragments (terminal restriction fragment length analysis). This technique provides an average telomere length from a population of cells, however it is limited by a lack of information on telomere length at a cellular or chromosomal level. Other telomere length measurement techniques make use of telomere-FISH PNA probes to label telomeric DNA and quantify the corresponding fluorescence as an estimation of telomere length. These include high throughput methods to measure the average telomere length per cell in a population of cells using flow cytometry (Flow-FISH), and quantitative

cytogenetic methods to measure telomere length at individual chromosome ends in metaphase chromosome spreads (Q-FISH). Another highly-specific PCR-based method measures the length of a single telomere (single telomere elongation length analysis, STELA).

While telomere-FISH PNA probes have been predominantly used for measuring telomere length, they can also be used to analyze telomeric DNA distribution in fixed cells or in metaphase chromosome spreads. This requires perforation of the nuclear membrane and low-ionic conditions to denature DNA-DNA interactions followed by re-annealing with the high binding affinity PNA probe. Consequently, this technique is not ideal for studying telomere dynamics in living cells.

1.12 Fluorescent proteins

A powerful method to study protein dynamics in living cells is to use molecular cloning techniques to fuse fluorescent proteins to a wide range of protein targets. Since the discovery of green fluorescent protein from the *Aequoria victoria* jellyfish in the 1960s [97], a wide range of fluorescent protein genetic variants have been developed with fluorescence emission profiles that span the visible and near-visible light spectrum (reviewed in [98]). By combining the use of fluorescent fusion proteins with multicolor live-cell fluorescence imaging, the dynamics of multiple protein targets can be visualized simultaneously in real-time.

1.13 Mouse embryonic stem cells

Mouse embryonic stem (ES) cells are derived from the inner cell mass of embryos at the blastocyst stage (day 3.5) and have the potential to differentiate into all of the specialised embryonic tissues. Undifferentiated mouse ES cells have the ability to renew themselves indefinitely under defined conditions. For instance, mouse ES cells can be maintained in an undifferentiated state in culture by growing cells in the presence of defined inhibitory factors to prevent differentiation, and by using a gelatin coated culture dish or a feeder layer of inactivated mouse embryonic fibroblasts to support adherent growth [99-101].

Since mouse ES cells give rise to the cells of the developing embryo, they must have mechanisms to maintain genomic integrity (reviewed in [102]). One mechanism may be the suppression of mutagenesis. Mouse ES cells exhibit mutation frequencies 100-fold lower compared to adult somatic cells or differentiated isogenic mouse embryonic fibroblasts [103, 104]. Another mechanism for the maintenance of genomic integrity is to preferentially use repair pathways which are error-free. DNA double-strand breaks can be repaired by two main pathways. Homologous recombination uses a template to guide repair of the break. This involves resection of the 5' ends of the break, followed by invasion of the 3' overhang into duplex DNA with a similar sequence. In contrast, non-homologous end joining (NHEJ) involves the direct ligation of broken ends and does not require a template. Since homologous recombination uses a template to repair DNA damage, it is relatively error-free, compared to NHEJ which is much more error-prone. Mouse ES cells spend the majority of cell cycle in S-phase and have a very

short G1 phase [105, 106]. Accordingly, the preferred pathway for DNA repair in mouse ES cells appears to be homologous recombination [107], which primarily occurs in S-phase and G2 when DNA replication provides a template for recombination. In contrast, NHEJ occurs primarily in G1, and does not appear to be a major DNA repair pathway in mouse ES cells [108, 109]. However, these mechanisms are not sufficient to maintain a stable genome in mouse ES cells.

Mouse ES cells divide rapidly (cell cycle time: ~8-12hr) and lack certain cell cycle checkpoints, presumably to generate the multitude of cells required for organism development [102, 110]. p53 is a tumour suppressor protein that functions to activate DNA repair proteins in response to DNA damage, and can induce a G1/S-phase cell cycle arrest, allowing cells time to repair DNA damage before continuing progression through the cell cycle. If DNA damage is not repaired efficiently, p53 can activate apoptosis (reviewed in [111]). Although studies have shown that mouse ES cells have higher cellular p53 protein levels compared to differentiated cells ([112], the majority of p53 protein is sequestered in the cytoplasm and does not efficiently enter the nucleus in the presence of DNA damage [105]. As a result, mouse ES cells can divide rapidly without activating the p53 checkpoint [105, 113]. It remains unclear why mouse ES cells, which presumably need to maintain a pristine genome, lack this major DNA damage checkpoint. However, studies have shown that damaged mouse ES cells undergo p53-independent apoptosis [105], suggesting that mouse ES cells with impaired genomes are removed from the population. Furthermore, the p53 checkpoint appears to be restored upon differentiation [105].

1.14 Project aims

In summary, telomeres are protective structures which distinguish the natural ends of linear chromosomes from DNA breaks. Telomeres have traditionally been studied in terms of telomere length regulation during aging and cancer. However, telomere associations have been observed during mitosis, meiosis and cancer which may represent an additional essential function for telomeres.

TRF1 protein levels appear to be highly regulated over the cell cycle. Furthermore, TRF1 has been implicated in mediating telomere associations, specifically at high TRF1 levels. We hypothesize that precise regulation of TRF1 protein levels is essential for telomere maintenance and cell cycle progression. In this thesis we aim to develop a system for visualizing telomere dynamics in real-time using live-cell fluorescence imaging of mouse ES cells. Using this system, we aim determine how defined levels of TRF1 protein influence telomere dynamics over the cell cycle. Our second aim is develop a system to directly test a potential mechanism for TRF1-mediated telomere associations. Our last aim is to investigate the cellular localization of RTEL1 in the presence of telomere dysfunction and DNA damage. We observed striking phenotypes linking TRF1 and RTEL1 at telomere associations, and propose a model for TRF1-mediated telomere associations in a cellular context.

Chapter 2: TRF1 overexpression induces telomere associations

2.1 Introduction

Although the traditional role of TRF1 has involved regulation of telomere length, TRF1 has been implicated as a potential candidate in mediating telomere associations. *In vitro* studies have shown that TRF1 protein alone can induce parallel pairing, and clustering of telomeric DNA tracts, specifically at high TRF1 protein levels [55]. It remains unclear whether TRF1 can mediate telomere associations in a cellular context.

We propose that precise regulation of TRF1 protein levels is essential for telomere maintenance and cell cycle progression. To determine telomere dynamics over the cell cycle, we generated mouse embryonic stem (ES) cells expressing TRF1 with and without a fluorescent protein tag. Mouse ES cells were chosen because they divide rapidly and can be easily transfected with a high transfection efficiency [114] to generate transient or stably expressing cell lines. Furthermore, mouse ES cells can be grown as adherent cells, which facilitates live-cell imaging by providing increased visualization of intracellular structures, and decreased cellular mobility.

To determine how defined TRF1 protein levels affect telomere dynamics over the cell cycle, we used using fluorescence-activated cell sorting (FACS) to obtain populations expressing defined levels of TRF1, and telomere dynamics were followed in real-time using live-cell fluorescence imaging. Telomere distribution was also analyzed in metaphase chromosome spreads. In this chapter, we describe a system to visualize telomere dynamics in real-time using fluorescently-tagged TRF1 fusion proteins. Using

this system we observed striking phenotypes during mitosis upon TRF1 overexpression, highlighting the importance of tight regulation of cellular TRF1 levels for telomere resolution and mitotic progression.

2.2 Results

2.2.1 Generating cell populations expressing defined TRF1 protein levels

To determine the effects of TRF1 overexpression on telomere dynamics, we overexpressed TRF1 in mouse ES cells. Constructs were generated encoding either *Trf1* fused to the C-terminus of Venus yellow fluorescent protein (YFP) [115], or *Trf1* co-transcribed, but translated separately from YFP by an internal ribosome entry site (IRES) ($TRF1_{IRES\text{-}YFP}$) (Figure 4A). These constructs allowed us to quantify relative levels of TRF1 expression in transfected cells and assess whether the N-terminal fusion affects TRF1 function. To obtain populations of cells expressing defined TRF1 protein levels, cells were transiently transfected with YFP-TRF1 or $TRF1_{IRES\text{-}YFP}$, and sorted by fluorescence-activated cell sorting (FACS) for low, medium, and high YFP levels at 24 hours post-transfection (Figure 4B). Compared to the low population, the medium and high population expressed 10-fold and ≥150 fold higher YFP levels, respectively (Figure 4B).

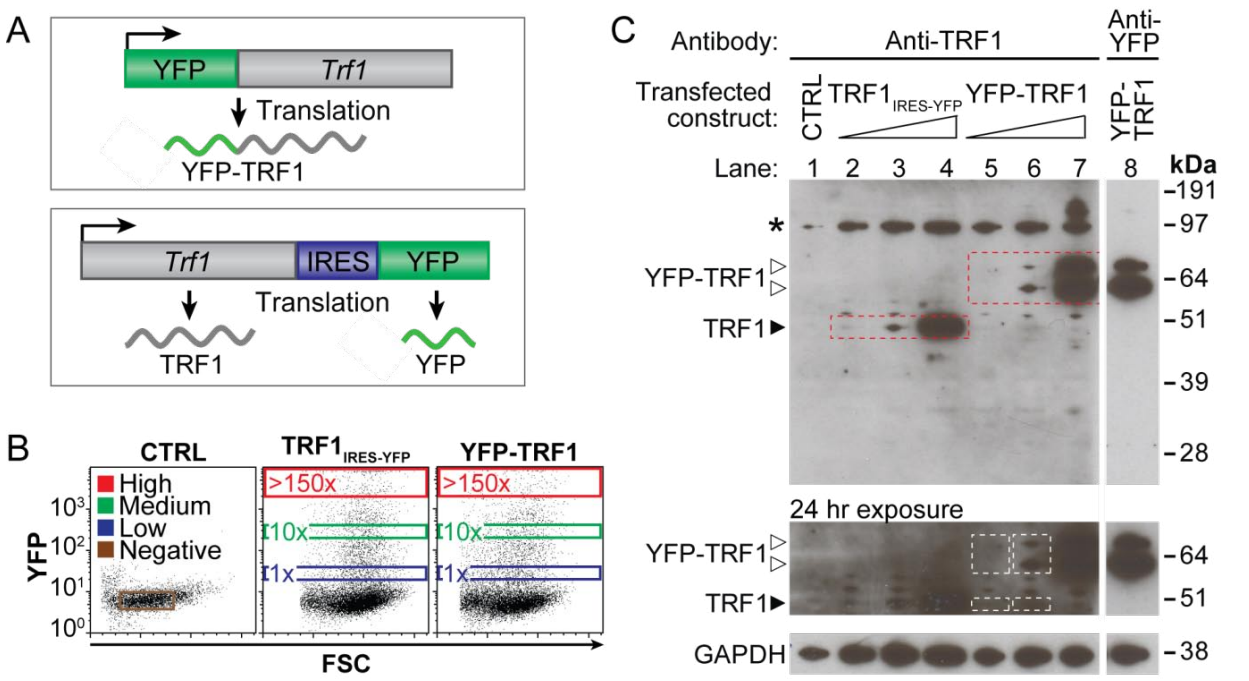

Figure 4. Generating cell populations expressing defined TRF1 protein levels.

(A) Schematic of constructs encoding YFP-TRF1 (top), and TRF1 translated separately from YFP by an IRES sequence (bottom). Constructs were driven by a CAG (CMV early enhancer/chicken beta-actin) promoter. (B) FACS plots showing untransfected control, cells transiently expressing $TRF1_{IRES\text{-}YFP}$ or YFP-TRF1 for 24 hours, and gates used for negative, low, medium, and high YFP levels. Numbers in gates indicate fold difference in median YFP levels compared to the low population. (C) Western blotting of sorted cell populations using an anti-TRF1 (lanes 1-7) or an anti-YFP (lane 8) antibody. Lane 1, mouse ES cells; lane 2-4, low, medium, and high $TRF1_{IRES\text{-}YFP}$; lane 5-7, low, medium, and high YFP-TRF1; lane 8, medium YFP-TRF1). The positions of TRF1 (solid arrowhead) and YFP-TRF1 doublet (open arrowheads) are indicated. Red boxes show increasing levels of $TRF1_{IRES\text{-}YFP}$ (lanes 2- 4) and YFP-TRF1 (lanes 5-7). Middle panel shows a 24 hour overexposure of the blot comparing endogenous TRF1 levels (lanes 5

and 6, lower white boxes) to low and medium YFP-TRF1 levels (lanes 5 and 6, upper white boxes). Non-specific labelling is indicated by asterisk. Lower panel shows glyceraldehyde 3-phosphate dehydrogenase (GAPDH) loading control.

To compare the levels of transfected TRF1 protein relative to endogenous TRF1 levels, Western blot analysis was performed using an antibody directed against TRF1. Endogenous TRF1 levels were difficult to detect by Western blot analysis (Figure 4C, lane 1). However, by analyzing populations expressing increasing levels of $TRF1_{IRES\text{-}YFP}$, we confirmed that TRF1 migrates at 50kDa (Figure 4C, solid arrowhead, red box) [54]. In populations expressing increasing levels of YFP-TRF1 we observed a doublet with a band at the expected molecular weight 77kDa, and an additional lower band at 60kDa (Figure 4C, open arrowheads, red box). This was confirmed with an antibody directed against YFP (Figure 4C, lane 8). It is not clear why two bands were observed. Our results, however, are consistent with previous studies showing that overexpressed green fluorescent protein (of which YFP is a variant) fusion proteins migrate as a doublet, where the molecular weight of the upper and lower bands in these previous studies corresponded to +27 and +10-15kDa higher than the nonfused protein, respectively [116, 117]. Other studies reported that doublet bands from GFP fusion proteins became single bands when higher concentrations of SDS (sodium dodecyl sulfate) were used [118]. SDS is a detergent that binds and unfolds proteins, giving them a uniform negative charge to mass ratio. It is possible that the SDS concentrations used in our experiments are not sufficient to properly unfold YFP in overexpressed fusion proteins, leading to differences in protein migration. Alternatively, YFP-TRF1

could be more stable than endogenous TRF1, leading to an accumulation of post-translationally modified proteins otherwise not detectable for the endogenous protein. Previous studies have shown that green fluorescent protein (of which YFP is a variant) can stabilize fluorescent fusion proteins, thus increasing the protein levels of the fusion protein within cells [119-121].

To visualize faint bands, the blot was exposed for 24 hours (Figure 4C, middle panel). In the low YFP-TRF1 population, YFP-TRF1 was roughly estimated to be half of endogenous TRF1 protein levels (Figure 4C, lane 5, white boxes), whereas in the medium YFP-TRF1 population, YFP-TRF1 was roughly estimated to be 5-fold higher than endogenous TRF1 protein levels (Figure 4C, lane 6, white boxes), based on densitometry. Although high YFP-TRF1 protein levels were quite saturated, extrapolation (YFP-TRF1 protein levels: endogenous 1x, low 0.5x, medium 5x) based on the gating from FACS (YFP-TRF1 fluorescence levels: low 1x, medium 10x, high >150x) indicates that the high YFP-TRF1 levels were >75x endogenous levels.

The YFP-TRF1 and the $TRF1_{IRES\text{-}YFP}$ populations had similar YFP levels as selected by FACS gating (Figure 4B, middle and right panel), and showed similar protein levels by western blot analysis (Figure 4C, lanes 2-4 and 5-7, red boxes). This observation suggests that YFP expression is a suitable indicator of TRF1 protein levels in both the N-terminal YFP fusion and the IRES strategies.

2.2.2 Telomere dynamics can be visualized by fluorescently labelled TRF1

YFP-TRF1-expressing cells gated for low YFP levels express the TRF1 fusion protein at levels comparable to endogenous TRF1. To determine whether the low YFP levels in this population can be used to track telomere organization during the cell cycle, low YFP-TRF1 cells were fixed and imaged in different stages of the cell cycle (Figure 5A) and followed by live-cell fluorescence imaging (Movie 1). In interphase, YFP-TRF1 foci are distributed throughout the entire nuclear volume. In metaphase, YFP-TRF1 foci clearly localize as doublets to sister-chromatid ends. In anaphase, TRF1 foci localize to the ends of segregating chromatids. These observations suggest that YFP-TRF1 correctly localizes to telomeres over the cell cycle and can be used to follow telomere dynamics in viable cells, in line with previous reports [56, 68].

To determine the number of telomere foci during the cell cycle, cells were fixed in suspension, and sorted by FACS into G1, S, and G2/M based on DAPI DNA content and immunostaining with a mitosis marker, anti-phospho-Histone H3 (Ser10) (Figure 5B). Image stacks were acquired using the same exposure and imaging conditions. Image analysis software was used to select YFP-TRF1 foci using the following steps. First, regions containing individual nuclei were selected using DAPI DNA staining. Second, we measured the average background fluorescence intensity from several different images as a percentage of the maximum intensity. Third, fluorescent foci above this threshold were selected for each nucleus and the number of foci per nucleus was determined.

As expected, individual foci that could be resolved nearly doubled from G1 to G2/M upon sister chromatid separation (Figure 5C), with numbers corresponding closely to the expected number of telomeres (diploid mouse cell: 80 telomeres in G1, and 160 in G2/M). The counted number of TRF1 foci was found to be slightly lower than expected, most likely due to an inability of the imaging system to resolve either very faint (short) telomeres or telomeres which are very close together. Taken together, these results support the idea that cells expressing low levels of YFP-TRF1 can be used to study the dynamic behaviour of telomeres in living cells.

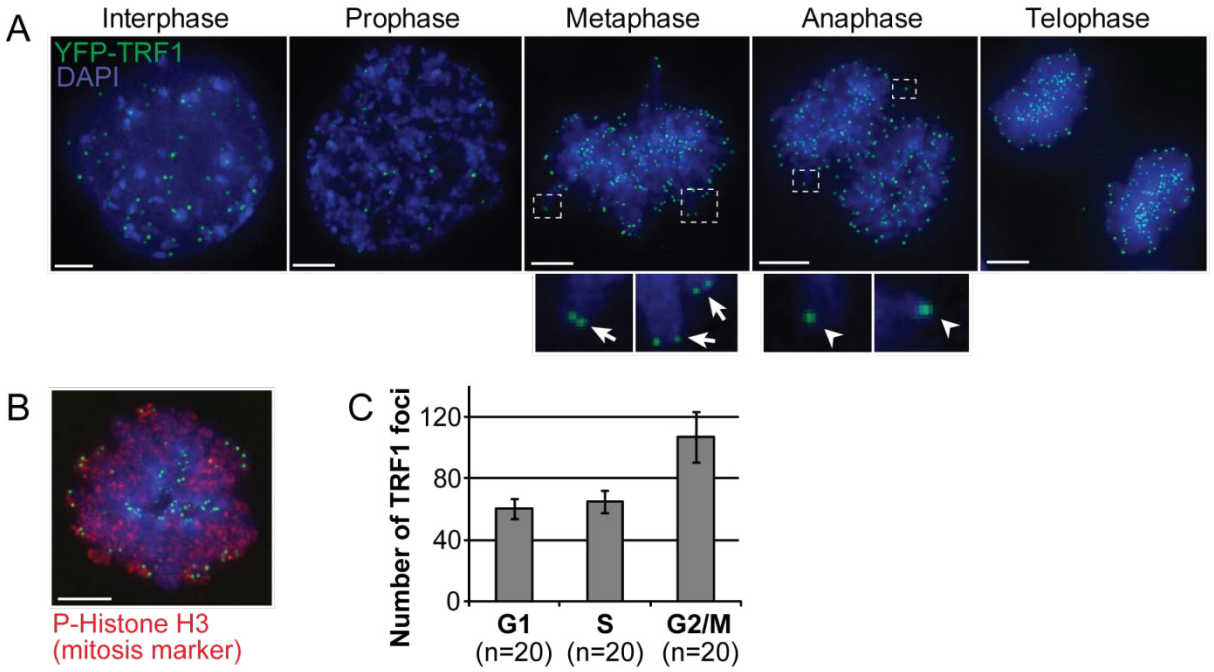

Figure 5. Telomere dynamics can be visualized by fluorescently labelled TRF1.
(A) Maximum intensity projection images of cells expressing low levels of YFP-TRF1 (green), population showing cellular localization over the cell cycle. DNA stain (blue). In metaphase, doublets of YFP-TRF1 foci are observed at sister-chromatid ends

(insets, arrows), whereas individual YFP-TRF1 foci are observed at the ends of segregating chromatids in anaphase (insets, arrowheads). (B) Projection image of a cell in metaphase immunostained with anti-phospho-Histone H3 (Ser10) mitosis marker (red). (C) Graph showing number of resolvable TRF1 foci per cell in G1, S and G2/M. Error bars, SD. Scale bar, 5 μM.

Movie 1. Telomere dynamics can be visualized by fluorescently labelled TRF1. Time-lapse movie showing mitosis in mouse ES cells expressing low levels of YFP-TRF1 (green) as well as H2B-RFP (chromosomes, red). Scale bar, 5 μM. See attached CD for movie.

2.2.3 TRF1 overexpression induces TRF1 bridges and TRF1 aggregates at telomeres

To obtain populations of cells with medium and high TRF1 expression levels, cells stably expressing low levels of YFP-TRF1 underwent a second round of transient transfection with YFP-TRF1 followed by sorting using FACS with gating as in Figure 4B. Live-cell fluorescence imaging was used to follow the sorted cells starting in metaphase through mitosis, at ~20-30 hours post-transfection and ~3-10 hours post-sorting. To visualize chromosomes, the cells also stably expressed Histone 2B (H2B) fused to the N-terminus of mCherry red fluorescent protein (RFP) [122]. Of the cells that entered anaphase from the medium YFP-TRF1 population, we found that the majority (71%) exhibited chromatin bridges containing several (~1-15) thin fibers of YFP-TRF1 connecting the chromosomes of segregating daughter cells (Figure 6A and Figure 6B,

and Movie 2). In contrast, none of the cells in the low YFP-TRF1 population exhibited chromatin bridges (Figure 6A and Figure 6B, and Movie 1).

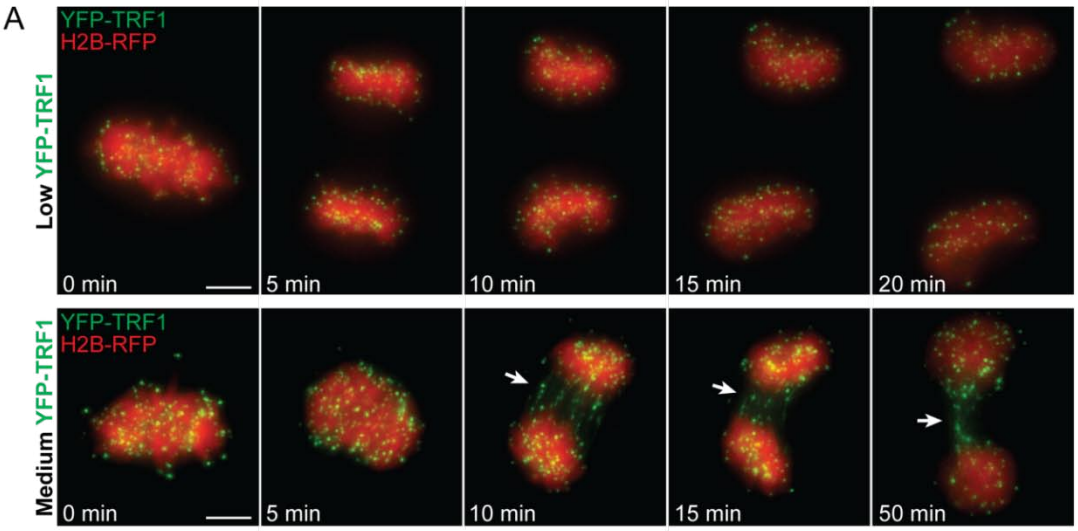

B

Sorted cell population	Total cells counted (starting in metaphase)	Cells proceeding to anaphase	Anaphase cells with YFP-TRF1 bridge	Mitotic bypass
Low YFP-TRF1	38	38	0 (0%)	0 (0%)
Medium YFP-TRF1	48	14	10 (71%)	36 (75%)

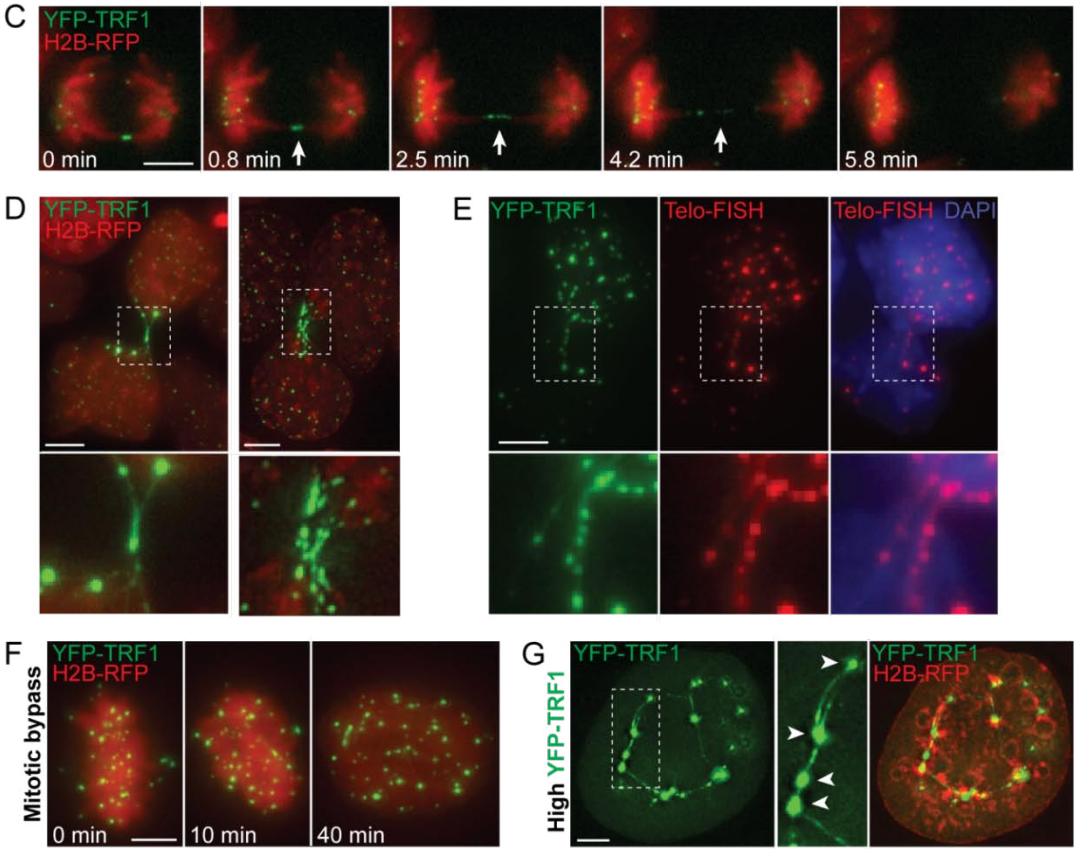

Figure 6. TRF1 overexpression induces anaphase bridges containing TRF1, mitotic bypass, and TRF1 aggregates.

Time-lapse images of cells expressing (A) low or (B) medium levels of YFP-TRF1 (green), and H2B-RFP (chromosomes, red). Note formation of YFP-TRF1 bridges (arrows) between segregating chromosomes in medium YFP-TRF1 expressing cells which persist into interphase. Images are maximum intensity projections. (B) Quantification of YFP-TRF1 bridges and mitotic bypass from two independent experiments. Percentages are given in brackets. (C) Time-lapse images showing transient chromatin bridge containing YFP-TRF1 (arrowhead). Note gradual lengthening and thinning of bridge over time (T=0 to T=4.2 min), until bridge is no longer visible (T=5.8 min). Images are of a single z-section. (D) Examples of persistent chromatin bridges containing multiple stretches of high local concentrations of YFP-TRF1 between daughter cells in interphase (insets). (E) YFP-TRF1 (green) foci overlap with telomere-FISH PNA probe (red) in chromatin bridges (insets). (F) Time-lapse images showing mitotic bypass. Note that this cell appears to progress from metaphase directly to interphase without undergoing cell division. (G) Example of an interphase cell expressing high YFP-TRF1 exhibiting several large, intense aggregates of YFP-TRF1 foci (arrowheads) connected by thin stretches of YFP-TRF1. Scale bar, 5 μM.

Movie 2. TRF1 overexpression induces TRF1 bridges between segregating chromosomes.

Time-lapse movie showing YFP-TRF1 bridges during mitosis in mouse ES cells expressing medium levels of YFP-TRF1 (green) and H2B-RFP (chromosomes, red).

Note that several thin fibers of YFP-TRF1 form between segregating chromosomes. Scale bar, 5 μM. See attached CD for movie.

Movie 3. Example of a transient YFP-TRF1 anaphase bridge.

Time-lapse movie showing transient YFP-TRF1 bridge. Note gradual lengthening and thinning of bridge over time, until bridge is no longer visible. Movie is of a single z-section. Scale bar, 5 μM. See attached CD for movie.

Bridges containing multiple fibers with high local concentrations of YFP-TRF1 often persisted between daughter cells into interphase (Figure 6A and Figure 6D). In contrast, we also observed cells with transient bridges containing a small number of thin fibers of YFP-TRF1, which appeared to gradually lengthen over time until the bridge was no longer visible, suggesting that the bridge may be resolved during mitosis (Figure 6C and Movie 3). These results suggest that the severity of the bridge determines the outcome of mitosis.

Since TRF1 proteins bind telomeric repeats [44], we reasoned that the TRF1 bridges likely contain telomeric DNA. To confirm this, cells grown on a slide were fixed and image stacks were acquired of chromatin bridges containing YFP-TRF1 at precise X-Y coordinates. Following hybridization with a telomere-FISH PNA probe to specifically label telomeric DNA, image stacks were acquired at the previously recorded X-Y coordinates. We observed that YFP-TRF1 bridges overlap closely with signals from the

telomere-FISH probe (Figure 6E), supporting the notion that chromatin bridges contain YFP-TRF1 protein as well as telomeric DNA.

TRF1 bridges were also induced by TRF1 alone, translated separately from the fluorescent protein label. In cells overexpressing $TRF1_{IRES\text{-}YFP}$ we observed a higher frequency (44.4%) of TRF1 bridges, compared to an IRES-YFP vector control (3.2%) (Figure 7). The observation that bridges can be induced by TRF1 alone suggests that the bridges observed in YFP-TRF1 overexpressing cells are not a dominant-negative effect from the fluorescent protein fusion to TRF1.

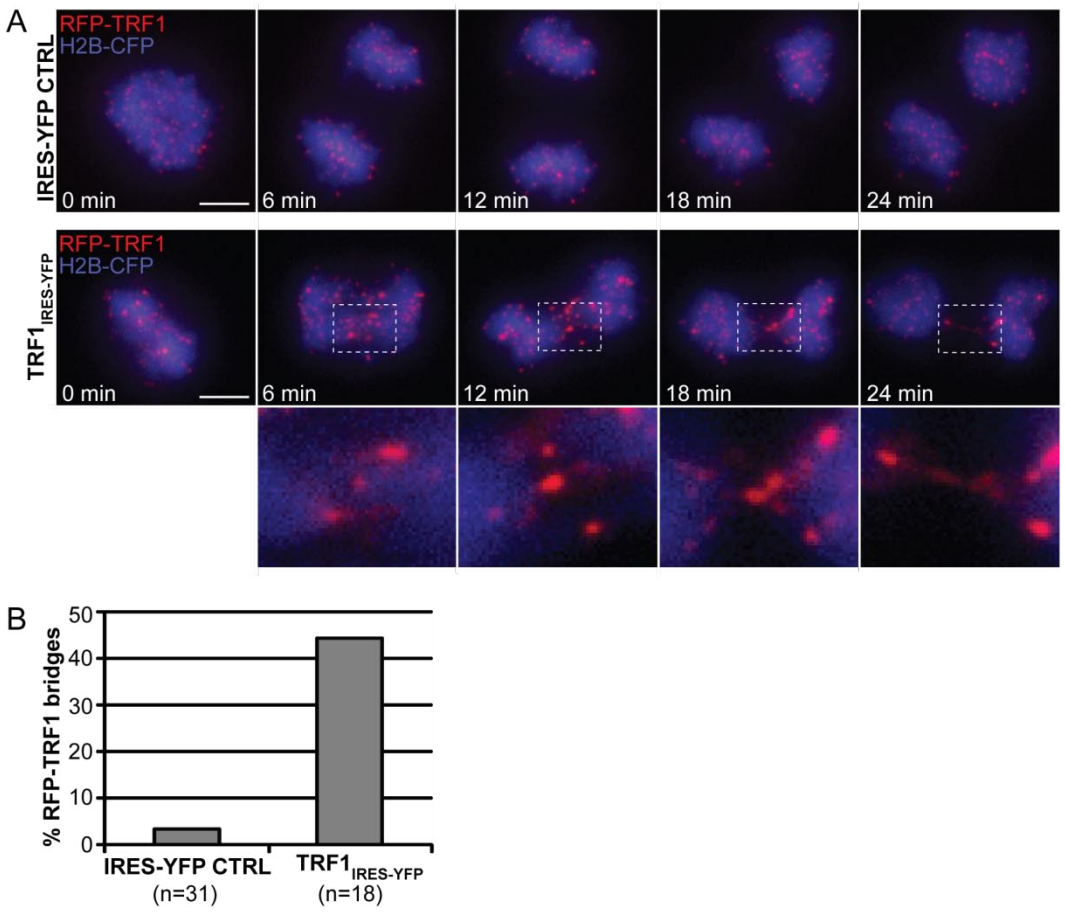

Figure 7. TRF1 bridges are induced by TRF1 alone.

(A) Time-lapse images of cells expressing medium YFP levels of IRES-YFP vector control (upper panel), or $TRF1_{IRES\text{-}YFP}$ (lower panel), starting in metaphase at ~24 hours post-transfection. To visualize telomeres and chromosomes, cells were stably expressing low levels of RFP-TRF1 (red), and H2B-CFP (blue). Since RFP-TRF1 was expressed at levels comparable to endogenous TRF1 (data not shown), we expect RFP-TRF1 to be used as an indicator of telomere distribution, and not induce bridges. Scale bar, 5 μM. (B) Quantification of RFP-TRF1 bridges.

2.2.4 TRF1 overexpression induces mitotic bypass

The majority (75%) of cells expressing medium levels of YFP-TRF1 bypassed mitosis, defined here as cells (starting in metaphase) failing to divide to form separate nuclei, and instead proceeding to form a single (tetraploid) nucleus in interphase with decondensed DNA (Figure 6B and Figure 6F). In contrast, none of the cells in the low YFP-TRF1 population underwent mitotic bypass. Of note, daughter cells in interphase that were still connected by persistent YFP-TRF1 bridges (Figure 6A and Figure 6D) were not included as having bypassed mitosis. However, cells with persistent YFP-TRF1 bridges were occasionally observed to undergo mitosis with alignment of chromosomes from both daughter cells onto a single metaphase plate, giving rise to tetraploid cells which often eventually underwent apoptosis (data not shown). This is in accord with previous studies, showing that persistent telomere dysfunction induces mitotic bypass and tetraploidy [123].

We also observed interphase cells with large aggregates of YFP-TRF1 connected by thin stretches of YFP-TRF1 (Figure 6G). This was predominantly observed in cells sorted for high YFP-TRF1 levels. These TRF1 aggregates were suggestive of telomere associations between multiple chromosomes.

2.2.5 TRF1 overexpression induces telomere associations

To determine the consequences of TRF1 overexpression for telomeres, metaphase chromosome spreads were prepared of mouse ES cells overexpressing $TRF1_{IRES\text{-}YFP}$, YFP-TRF1, and an IRES-YFP control. To increase the yield of metaphase spreads, FACS gates for sorting were set to include cells with medium or higher YFP levels. Telomeres were labelled using a telomere-specific FISH probe. During a normal cell cycle, sister telomeres are resolved into distinct foci. We observed single or joined sister telomeres at the long-arm in up to 15% of telomeres in $TRF1_{IRES\text{-}YFP}$ overexpressing cells (Figure 8B and Figure 8C). In contrast, single and joined telomeres were less frequent (<1%) in IRES-YFP control cells (Figure 8A). Occasionally, we observed telomere associations between telomeres from different chromosomes in $TRF1_{IRES\text{-}YFP}$ overexpressing cells (Figure 8D). This was more pronounced in YFP-TRF1-overexpressing cells in which large, intense aggregates of telomere foci were observed, indicating that telomeres from different chromosomes were joined (Figure 8E). Each telomere aggregate was surrounded by multiple (up to 7) radially distributed chromosomes. These results suggest that TRF1 overexpression can induce two forms of telomere associations, single or joined sister telomeres, as well as telomere aggregates between multiple chromosomes.

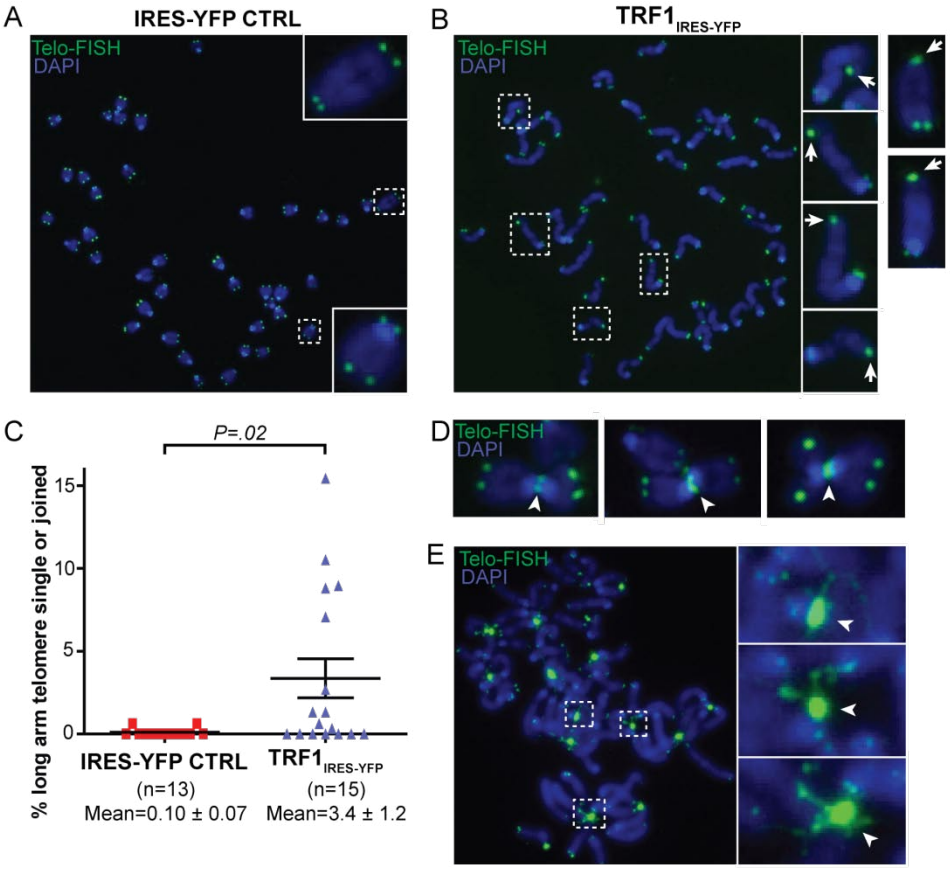

Figure 8. TRF1 overexpression induces telomere associations.

Examples of metaphase chromosome spreads in mouse ES cells transiently expressing medium to high levels of (A) vector control (IRES-YFP) or (B) $TRF1_{IRES\text{-}YFP}$ at ~72h post-transfection. Telomeres were labelled by a telomere-FISH PNA probe conjugated to Cy5 (green), and DNA was stained with DAPI (blue). (C) Column scatter plot showing percent of single or joined telomeres at long-arm. The p-value was calculated using an unpaired two-tailed t test. Mean +/- SEM is indicated. (D) Examples of telomere associations between metaphase chromosomes (arrowheads) in $TRF1_{IRES\text{-}YFP}$ overexpressing cells and (E) YFP-TRF1 overexpressing cells at ~72h post-transfection. Insets show telomere aggregates where each telomere aggregate

is surrounded by multiple (up to 7) radially distributed chromosomes. Gamma correction of histogram fluorescence levels was set to 0.5 for images in (E) to visualize lower intensity signals.

2.3 Discussion

Previous *in vitro* studies have implicated TRF1 as a potential candidate in mediating telomere associations. Consistent with these studies, we observed telomere associations and telomere segregation defects during mitosis in TRF1-overexpressing cells, indicating that telomeres were not fully resolved prior to cell division. Telomere associations were observed using two different forms of TRF1, with and without an N-terminal fluorescent tag, suggesting that the phenotypes we observed were not a dominant-negative effect from the fluorescent protein fusion to TRF1. Significantly, the severity of the telomere association phenotypes appeared to be related to the level of TRF1 protein in the cell. This suggests that tight regulation of TRF1 protein levels is essential for resolution of telomeres, specifically during mitosis.

We find that TRF1 overexpression (at >10-fold endogenous TRF1 levels) leads to TRF1 bridges at telomeric DNA. We observed both transient bridges, which resolved during mitosis, and persistent bridges, which remain between daughter cells in interphase. These observations suggest that the severity of the bridge determines the outcome of mitosis. Telomere associations appear to form preferentially at elevated levels of TRF1, presumably when the ratio of telomere binding sites is limiting compared to TRF1 levels.

We observed two classes of telomere associations, between sister telomeres and between telomeres from different chromosomes. This is consistent with previous *in vitro* studies showing that moderate TRF1 concentrations (2 monomers per telomere repeat) lead to parallel pairing of DNA probes containing tracts of telomeric DNA, while high TRF1 concentrations (>5 monomers per telomere repeat) lead to aggregates containing many DNA molecules [55]. Furthermore, the parallel orientation of the DNA tracts in these experiments is consistent with the parallel orientation of sister-telomeres, or telomeres from chromosomes aligned side-by-side. Of note, TRF1 alone was sufficient to induce DNA tract pairing and aggregation in these *in vitro* studies, suggesting that TRF1 protein alone can directly induce telomere associations.

Long-term TRF1 overexpression in stably expressing telomerase-positive human tumour cell line resulted in gradual telomere shortening [57]. However, these experiments were done over 124 population doublings (PDs). In contrast, our experiments using telomerase-positive mouse ES cells transiently overexpressing TRF1 were performed in a much shorter time frame of ~1-5 PDs. Furthermore, mouse ES cells have relatively long telomeres (~54kb) and significant telomere shortening by the end replication problem is not likely to occur in the short time frame of our experiments. Due to the difficulty in distinguishing individual chromosome ends in telomere aggregates involving a number of radially-distributed metaphase chromosomes, it was technically challenging to determine the telomere length of individual chromosomes ends in these experiments.

Although telomere associations and TRF1 anaphase bridges were observed upon overexpression of TRF1 with and without an N-terminal fluorescent tag, the phenotypes induced by $TRF1_{IRES\text{-}YFP}$ did not appear to be as severe as in YFP-TRF1 cells. Large telomere aggregates involving several different chromosomes were frequently observed in YFP-TRF1-overexpressing cells, but telomere associations between different chromosomes were only occasionally observed in $TRF1_{IRES\text{-}YFP}$-overexpressing cells. It is possible that the YFP-TRF1 fusion protein induces more penetrant phenotypes, due to increased stabilization of the fusion protein by YFP [119-121].

We found that the majority of mouse ES cells exhibited a mitotic block and underwent mitotic bypass, proceeding directly to interphase without dividing. However, a significant number of mouse ES cells were able to proceed through anaphase in the presence of unresolved telomeres, giving rise to telomere bridging. In contrast, the predominant phenotype in an immortalized human tumor cell line (HeLa) upon tankyrase 1 depletion was a mitotic arrest in early anaphase with unresolved sister-telomeres and cells did not proceed through anaphase [65, 78, 79]. Further studies are required to determine why certain cells exhibit different responses to telomere dysfunction. It is possible that rapidly dividing undifferentiated mouse ES cells have a higher threshold for telomere dysfunction than somatic human cells, due to the longer telomeres or undifferentiated state of mouse ES cells [105]. Note that both HeLa and mouse ES cells are telomerase-positive and have deficient p53 checkpoint pathways [105, 113, 124, 125], suggesting that these factors are not responsible for the

differences in response to telomere dysfunction. Future experiments could involve comparing the response to telomere dysfunction in undifferentiated and differentiated cells.

Telomere associations may be mediated by protein interactions or DNA interactions. One method that has been used as a rough indicator of protein interactions is treatment with a hypotonic solution. Hypotonic treatment is an essential step in the preparation of good quality metaphase chromosome spreads, which induces swelling of the nucleus and spreading of chromosomes [126]. Studies have reported that hypotonic treatment releases some but not all proteins from chromosomes, based on the observation that certain proteins cannot be visualized by immunostaining following hypotonic treatment. Despite using hypotonic treatment in our preparation of metaphase chromosome spreads, we observed a subset of $TRF1_{IRES\text{-}YFP}$-overexpressing cells with up to 15% of sister telomeres associated. However, we also observed a subset of cells with low to no sister telomere associations. In comparison, hypotonic treatment was sufficient to resolve sister telomere associations in tankyrase 1-depleted cells, leading to the proposal that telomere associations are mediated by a protein interaction [78]. However, hypotonic treatment is an indirect method to test for protein interactions and it is not clear how efficiently proteins are removed using this method. In the next chapter, we outline experiments designed to more directly examine how telomere-specific proteins might mediate telomere associations.

Chapter 3: Resolution of telomere aggregates by TRF1 cleavage

3.1 Introduction

Since we observed in Chapter 2 that TRF1 overexpression results in sister telomere associations and telomere aggregates, we hypothesized that TRF1 is physically involved in the joining of telomeres in our overexpression model. Previously, a mechanism was proposed whereby telomere-specific proteins mediate cohesion between sister telomeres [78, 87], which could function to physically link sister telomeres together from replication until mitosis, in a similar manner to cohesin complexes which link together sister chromatids at centromeres and along chromosome arms.

Telomere associations may be caused by protein-mediated interactions or DNA-mediated interactions. Protein-mediated interactions can form by two main mechanisms, proteins which physically bind DNA to form a protein bridge linking DNA strands, or proteins which form a ring structure encircling DNA strands. A wealth of literature exists on potential mechanisms for protein-mediated association of duplex DNA, generally involving combinations of these two mechanisms, and variations on the number of proteins directly and non-directly involved (reviewed in [127, 128]). In contrast, DNA-mediated interactions can arise via processes such as recombination, telomere fusion, stalled telomere replication or DNA catenation.

An assay that has previously been used to distinguish between protein-mediated and DNA mediated interactions, involves a highly-specific protease from the tobacco etch virus (TEV) that cleaves proteins engineered to contain a specific seven-amino acid TEV protease recognition site [129]. Studies in yeast and *Drosophila* have tested the ring structure of cohesin by using TEV protease to cleave cohesin at various sites within the proposed cohesin ring, which induced the separation of sister-chromatids in metaphase [129, 130]. TEV protease-mediated protein cleavage is a powerful tool to study protein function because it rapidly cleaves proteins at a specific site that is not typically present in proteins of mammalian cells [131, 132]. In contrast, techniques that interfere with the synthesis of proteins, such as siRNA, can be limited by sequence specificity and the time required for gradual depletion of the protein (reviewed in [133]).

Looking closer at the structure of TRF1 provides clues as to how TRF1 might mediate telomere cohesion. TRF1 contains an unstructured flexible linker domain, which connects the dimerization domain and the Myb DNA-binding domain [4]. Due to the flexibility and variable binding of TRF1 [4, 40], TRF1 has been proposed to bind telomeres in different conformations, such as a *cis* conformation with each Myb DNA-binding domain binding adjacent sites on the same telomere, or in a *trans* conformation with each Myb DNA-binding domain binding sites that are far apart or on opposing telomeres (Figure 9). Evidence supporting the existence of *trans*-TRF1 *in vitro* demonstrated that TRF1 induced looping of telomeric DNA tracts, specifically when available binding sites were limited to two Myb DNA-binding sites placed far apart on the same DNA tract [4]. Notably, TRF1 protein was observed at the junction of the loop,

which was consistent with the size of one TRF1 dimer, suggesting that a single TRF1 dimer is sufficient to induce associations between telomeric DNA.

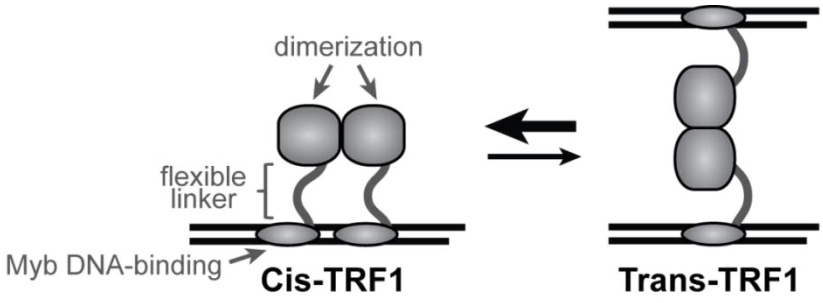

Figure 9. Proposed mode of binding for flexible TRF1 dimers at telomeres. a) showing the *cis* and *trans* conformation. The *cis* and *trans* conformation may exist in equilibrium with the *cis* conformation usually being the most energetically favourable (Modified from Bianchi et al. 1999).

We propose that the telomere associations induced by TRF1 overexpression which we observed in the previous chapter may be the direct result of TRF1 proteins physically bridging telomeres together, as opposed to being formed by DNA interactions. One potential mechanism by which TRF1 could mediate telomere associations is by physically bridging telomeres together in a *trans* conformation. If telomere associations are mediated by TRF1 physically bridging telomeres together, then we reason that cleavage of TRF1 protein would resolve telomere associations. In this chapter, we describe the development of an assay for TEV protease-mediated cleavage of TRF1 dimers in mammalian cells, which can be combined with live-cell imaging for real-time visualization of telomere dynamics upon TRF1 cleavage.

3.2 Results

3.2.1 Generating cell populations for TRF1 cleavage assay

To make TRF1 protein cleavable, a TEV protease recognition site was inserted in the flexible linker of TRF1, and this was fused to YFP (YFP-$TRF1_{TEV}$) (Figure 10A). The flexible linker is poorly conserved and therefore this cleavable TRF1 protein should bind telomeres normally prior to induction of TRF1 cleavage with TEV protease. YFP-$TRF1_{TEV}$ was also fused to a degradation domain (FKBP, FK506 binding protein) which can be stabilized upon addition of a synthetic ligand known as Shield-1 [134], for inducible expression of cleavable TRF1. We generated a stable clone expressing low levels of YFP-$TRF1_{TEV}$ and transiently transfected these cells a second time with YFP-$TRF1_{TEV}$ in the presence of Shield-1 to overexpress and stabilize the cleavable YFP-$TRF1_{TEV}$ protein. Note that a second transient transfection with YFP-$TRF1_{TEV}$ was required most likely because not enough of the overexpressed YFP-$TRF1_{TEV}$ was stabilized by Shield-1 to induce telomere aggregates in the stable clone. Cells were then sorted for high levels of YFP-$TRF1_{TEV}$ (FACS gating was the same as in Figure 4B, high gate) to be imaged at 24-48 hours post-transfection and ~3-10 hours post-sorting. TRF1 cleavage was induced by transient transfection with TEV protease fused to Cerulean cyan fluorescent protein (CFP) [135], driven by a CAG promoter (Figure 10A). In addition, nuclear localization signals were fused to the N and C-terminus of TEV Protease, which has been reported to facilitate nuclear entry [130]. To visualize telomeres before and after detection of CFP-TEV protease, cells were also stably expressing low levels of non-cleavable RFP-TRF1 (Figure 10A). Since RFP-TRF1 was expressed at levels comparable to endogenous TRF1 (data not shown), we expected

that RFP-TRF1 could be used as a faithful indicator of telomere distribution, and it would that not induce telomere aggregates by itself.

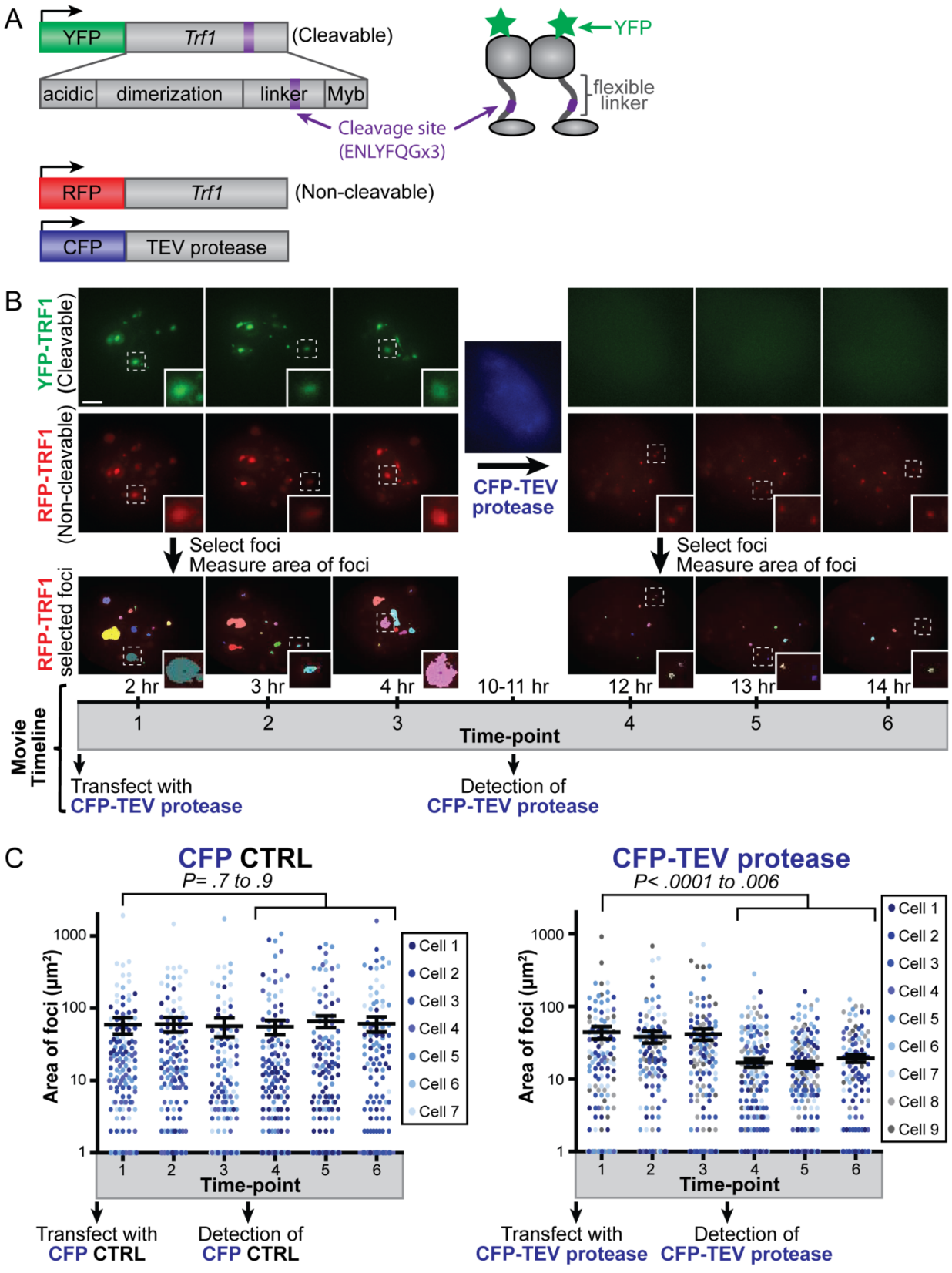

Figure 10. Resolution of telomere aggregates by TRF1 cleavage.

(A) Schematic of constructs used for TRF1 cleavage assay, including cleavable YFP-TRF1$_{TEV}$ showing TRF1 domains with TEV cleavage site (purple) inserted in flexible hinge domain, non-cleavable RFP-TRF1 to visualize telomeres, and CFP-TEV protease driven by a CAG promoter to cleave the YFP-TRF1$_{TEV}$. (B) Projection images of cells expressing high levels of cleavable YFP-TRF1$_{TEV}$ (green) and low levels of non-cleavable RFP-TRF1 (red) for three time-points before and after detection of CFP-TEV protease (blue). Note that upon detection of nuclear CFP-TEV protease, cleavable YFP-TRF1$_{TEV}$ becomes diffuse, and non-cleavable RFP-TRF1 foci are smaller and more uniform (insets). Examples of RFP-TRF1 foci selected using automatic thresholding of fluorescence intensity are shown (bottom panel), where each color represents one selected focus. (C) Column scatter plot showing area of foci on a log scale, for three time-points before and after detection of CFP-TEV protease or CFP control, where each dot represents one selected focus. Time-lapse movies of nine and seven individual cells are represented for CFP-TEV protease and CFP control, respectively (legend). The number of foci represented for CFP-TEV protease was n=124, 138, 143, 202, 198, 124, and for CFP control was n=136, 121, 114, 151, 130, 141 for time-points 1 to 6, respectively. P-values for T=1 compared to a range of T=4 to 6 is shown, and was calculated using an unpaired two-tailed t test. Error bars, SEM. Scale bar, 5 μM.

Movie 4. Resolution of telomere aggregates by TRF1 cleavage (CFP).

Movie 5. Resolution of telomere aggregates by TRF1 cleavage (YFP).

Movie 6. Resolution of telomere aggregates by TRF1 cleavage (RFP).

Movie 7. Resolution of telomere aggregates by TRF1 cleavage (YFP and RFP).

Movie 8. Resolution of telomere aggregates by TRF1 cleavage (Bright field). Time-lapse movie of mouse ES cells expressing high levels of cleavable YFP-$TRF1_{TEV}$ (green) and low levels of non-cleavable RFP-TRF1 (red) upon detection of CFP-TEV protease (blue) driven by a CAG promoter. Note that upon detection of CFP-TEV protease, YFP-$TRF1_{TEV}$ fluorescence becomes diffuse, indicating that cleavage has occurred. The cell appears to divide at T=7-8 hr (bright field). Scale bar, 5 μM. See attached CD for movies.

3.2.2 Telomere aggregates are resolved by TRF1 cleavage

To visualize TRF1 cleavage in real-time, cells stably expressing low levels of non-cleavable RFP-TRF1 (red), and expressing high levels of cleavable YFP-$TRF1_{TEV}$ (green) were transiently transfected with CFP-TEV protease (blue) or a CFP only control (Figure 10A), and followed by live-cell fluorescence imaging (Movies 4-8). Before detection of CFP-TEV protease, large aggregates of TRF1 foci were observed as overlapping signals in both the YFP and RFP fluorescence channels, indicating that both the cleavable (green) and non-cleavable (red) TRF1 fusion proteins co-localize (Figure 10B, time-points 1 to 3). The detection of nuclear CFP (blue) fluorescence indicated successful expression and nuclear entry of CFP-TEV protease (Figure 10B). If TRF1 cleavage is successful, we expect that the cleaved N-terminal portion of YFP-$TRF1_{TEV}$ will no longer be directly linked to the telomere via the C-terminal DNA-binding domain. Indeed, we observed a distinct change in YFP localization from distinct foci to a diffuse fluorescence, which occurred at the same time as detection of CFP-TEV

protease (Figure 10B). This suggests that both the detection of CFP-TEV protease and diffuse YFP localization can serve as timing indicators of TRF1 cleavage.

Since RFP-TRF1 indicates telomere distribution within the cells, we can monitor the extent of telomere aggregates before and after detection of CFP-TEV protease. Images were acquired for in individual cells for three time-points before and after detection of CFP-TEV protease (Figure 10B). RFP-TRF1 foci were selected using automatic thresholding of fluorescence intensity and the area of each focus was measured (Figure 10B, lower images). Following detection of CFP-TEV protease, RFP-TRF1 foci were smaller and more uniform (Figure 10B, insets, and Figure 10C, right). We also visually observed an increase in the number of foci after TRF1 cleavage, although not all foci could be detected above background fluorescence by automatic thresholding (Figure 10B). In contrast, cells transfected with a CFP control did not show a significant change in the area (Figure 10C, left) or number of foci. Notably, we observed that cells often underwent mitosis upon detection of CFP-TEV protease, suggesting that upon TRF1 cleavage, cells were released from a mitotic block and resumed cell cycle progression (Movies 4-8).

We observed that a few hours after detection of CFP-TEV protease driven by a CAG promoter, cells exhibited mild toxic effects, such as nuclear blebbing indicative of apoptosis. We next sought to determine how CFP-TEV protease driven by a lower expressing PGK promoter (phosphoglycerate kinase) would affect telomere resolution. It was technically challenging to image PGK CFP-TEV protease due to the high energy light exposure required to detect the low levels of CFP fluorescence. However, the change in fluorescence of YFP-TRF1$_{TEV}$ from distinct foci to a diffuse fluorescence served as a timing indicator of TRF1 cleavage. We observed that the YFP-TRF1$_{TEV}$ fluorescence became gradually diffuse at a slower rate compared to previous experiments with the CAG CFP-TEV protease. This corresponded temporally with a significant change in non-cleavable RFP-TRF1 localization, where we observed a dramatic increase in foci number and a decrease in foci size (Figure 11 and Movies 9-11). This suggests that TRF1-mediated telomere aggregates are resolved more slowly and thoroughly when CFP-TEV protease is expressed at lower levels.

Taken together, these results suggest that TRF1-overexpression-induced telomere aggregates are mediated by TRF1, and that cleavage of TRF1 dimers resolves telomere associations and allows cell cycle progression.

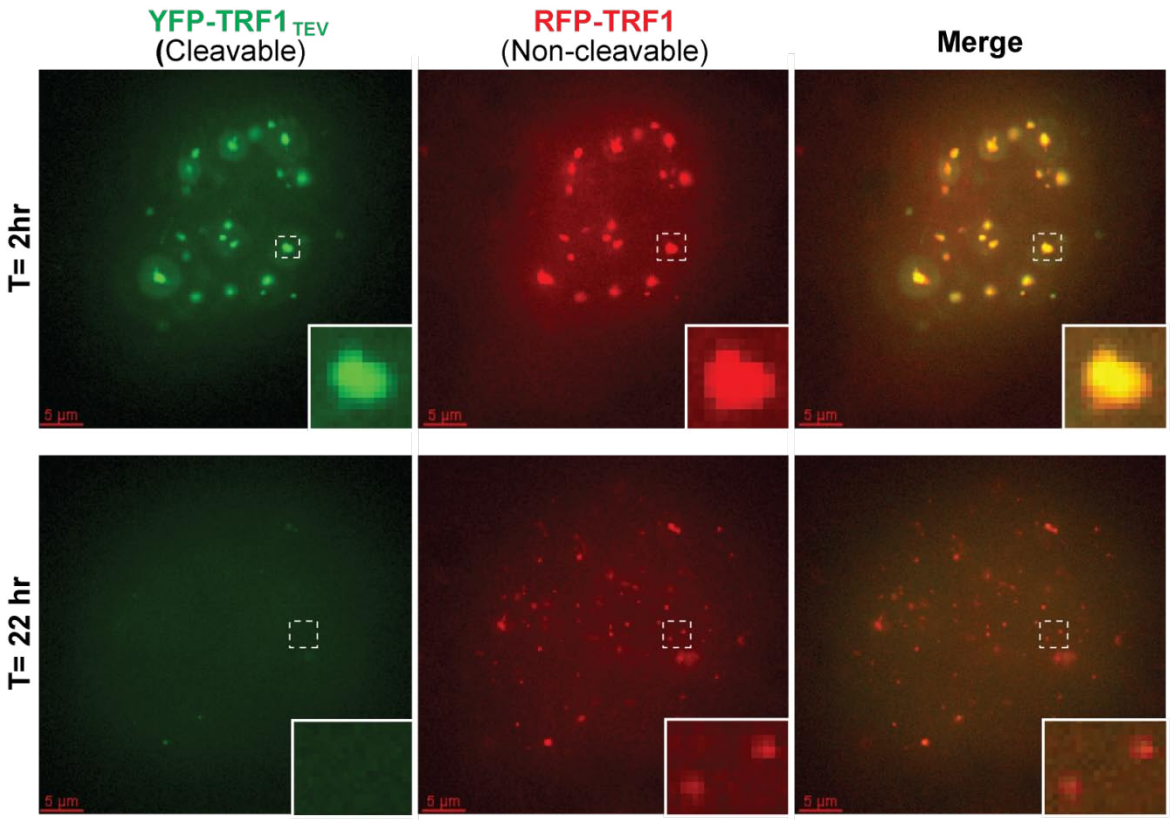

Figure 11. Gradual resolution of telomere aggregates by TRF1 cleavage.

Projection images from a time-lapse movie of cells expressing high levels of cleavable YFP-TRF1$_{TEV}$ (green) and low levels of non-cleavable RFP-TRF1 (red) upon transfection with CFP-TEV protease driven by a low expressing PGK promoter. Time (T=) indicates time after transfection of PGK CFP-TEV protease. Note that YFP-TRF1$_{TEV}$ fluorescence becomes diffuse (indicating that cleavage has occurred), and non-cleavable RFP-TRF1 aggregates become smaller and more uniform (insets). Scale bar, 5 µM.

Movie 9. Gradual resolution of telomere aggregates by TRF1 cleavage (YFP).

Movie 10. Gradual resolution of telomere aggregates by TRF1 cleavage (RFP).

Movie 11. Gradual resolution of telomere aggregates by TRF1 cleavage (Merge).

Time-lapse movie of mouse ES cells expressing high levels of cleavable YFP-$TRF1_{TEV}$ (green) and low levels of non-cleavable RFP-TRF1 (red) upon transfection with CFP-TEV protease driven by a low expressing PGK promoter. As YFP-$TRF1_{TEV}$ fluorescence gradually becomes diffuse (indicating that cleavage has occurred), non-cleavable RFP-TRF1 aggregates become smaller and more uniform. Scale bar, 5 μM. See attached CD for movies.

3.3 Discussion

We have developed a novel assay that combines site-specific protein cleavage by TEV protease with live-cell fluorescence imaging in mammalian cells to study the role of TRF1 in telomere associations. Our results suggest that telomere aggregates in cells that overexpress TRF1 can be resolved by cleavage of the TRF1 protein, suggesting that the telomeres in such cells are not resulting from DNA-mediated interactions but primarily from TRF1-mediated protein interactions.

One potential mechanism by which TRF1 could mediate telomere associations is by physically bridging telomeres together in a *trans* conformation. This is based on two key findings from studies using electron microscopy. First, these studies showed that TRF1 protein alone was sufficient to induce associations between telomeric DNA tracts, specifically at high TRF1 protein concentrations [55]. Second, a protein ball consistent with the size of a single TRF1 dimer was sufficient to induce looping of telomeric DNA

tracts, when available binding sites were limited to two Myb DNA-binding sites placed far apart [4]. Our results suggest that elevated levels of TRF1 protein can also induce telomere associations in a cellular context. Based on these findings, we propose that when telomere binding sites are limiting relative to the TRF1 protein levels in a cell, competition for binding sites can result in TRF1 dimers binding in a *trans* conformation (Figure 12, left).

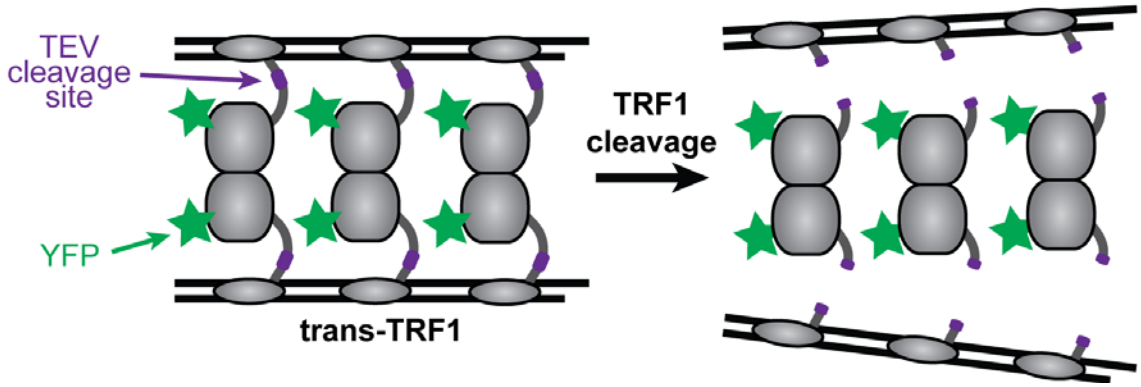

Figure 12. Model for TRF1-mediated telomere associations.

Potential mechanism showing two telomeric DNA strands associated by multiple TRF1 dimers in *trans* before and after TRF1 cleavage. See text for discussion.

By using both cleavable TRF1 (at elevated levels) to induce telomere associations, and non-cleavable TRF1 (at low levels) to visualize telomeres, we were able to visualize the dynamics of telomere resolution upon TRF1 cleavage in real-time using live-cell imaging. We observed that telomere aggregates decreased in size at the same time as detection of TEV protease in TRF1-overexpressing cells, suggesting that telomere aggregates were resolved by cleavage of the TRF1 protein. Furthermore telomere

aggregates appeared to resolve more slowly and thoroughly when CFP-TEV protease was expressed at lower levels.

Although an overall increase in foci number was observed visually, not all foci could be detected above background fluorescence by automatic thresholding, most likely due to the low expression levels of non-cleavable TRF1. It is not clear from our experiments whether the cleaved portion of TRF1 containing the Myb domain still binds telomeric repeats. In vitro studies have shown that TRF1 dimers require both Myb domains for stable binding to DNA [42], suggesting that the cleaved Myb domain has decreased telomere binding affinity. Although the cleaved Myb domain may interfere with the binding of non-cleavable TRF1, TRF1 binding to telomeres is dynamic with a high turnover rate (25s half-life) [68], suggesting that telomere binding of the non-cleavable TRF1 would likely have reached an equilibrium in the time frame of our experiments.

We anticipated that TRF1 cleavage would resolve TRF1 bridges, in addition to resolving telomere aggregates. However, experiments examining the outcome of TRF1 bridges upon TRF1 cleavage proved to be technically challenging. As described in Chapter 2, TRF1 bridges were often short-lived and appeared to gradually resolve during mitosis. Consequently, it was difficult to distinguish between TRF1 bridges that were resolved as a cellular outcome, and TRF1 bridges that were resolved by TRF1 cleavage. Although persistent bridges were longer-lived, they were only observed at a low frequency, which was technically challenging to combine with TRF1 cleavage

induced by transient expression of TEV protease. In chapter 6 we discuss potential future experiments to overcome these challenges. Although the TRF1 cleavage assay can be used to show how cleavage of TRF1 protein affects resolution of telomere aggregates, our studies alone cannot exclude additional contributing factors, such as the conformation of TRF1, TRF1 multimerization with other TRF1 dimers, or the effect of other proteins at telomeres. These contributing factors are also further discussed in chapter 6.

In the next chapter we investigate the cellular localization of an essential helicase that may be specifically recruited to resolve telomere associations.

Chapter 4: RTEL1 recruitment to TRF1 bridges at telomeres and sites of DNA repair

4.1 Introduction

We observed telomere associations and segregation defects in Chapter 2. We sought to determine whether certain proteins might be recruited to resolve or repair these telomere associations. A good candidate is the helicase RTEL1 which has functions in telomere maintenance and DNA repair. RTEL1-deficient cells exhibit telomere shortening, impaired cell growth, and chromosome breaks and fusions (Ding et al., 2004). RTEL1 has also been shown to suppress homologous recombination during DNA repair [89].

Evidence linking RTEL1 and TRF1 at telomeres demonstrated that both these proteins are required to suppress aberrant fragile phenotypes at telomeres, indicative of specific chromosome regions which are especially sensitive to replication stress [93]. Based on these studies, RTEL1 was proposed to be recruited to telomeres by TRF1, possibly to resolve higher-order structures which can form at telomeres [28, 89, 93, 95]. However direct evidence showing RTEL1 recruitment to telomeres is lacking. RTEL1 localization has been described as nuclear with a fine granular staining [28], however the cellular localization of RTEL1 in the presence of DNA damage or telomere dysfunction is unclear. Previous studies attempting to visualize RTEL1 have been limited by low levels of endogenous RTEL1 in cells, and toxicity caused by RTEL1 overexpression. In this chapter, we use live-cell fluorescence imaging to characterize

the cellular localization of inducible RTEL1 upon treatment with various DNA damaging agents or in the presence of elevated levels of TRF1.

4.2 Results

4.2.1 RTEL1 cellular localization is nuclear

To investigate the cellular localization of RTEL1, we generated RTEL1-deficient mES cell lines stably expressing low levels of inducible RTEL1 fused to YFP and an FKBP degradation domain (RTEL1-YFP) [134]. These cells were grown in the presence of the FKBP-stabilizing ligand Shield-1 (1 μM) for 24-48 hours prior to live-cell imaging to stabilize RTEL1 protein. Using this approach we were able to visualize the cellular localization of RTEL1. However, we observed that RTEL1-YFP was highly sensitive to photobleaching and fluorescence was significantly diminished following the acquisition of a single image, likely due to the low levels of RTEL1 expression. Accordingly, we found that it was important to minimize light exposure to cells prior to imaging and carefully optimize imaging conditions. Cells were able to undergo numerous (up to 25) cell passages following stabilization of RTEL1 without any apparent abnormalities in cell growth or morphology, suggesting that the low levels of exogenous RTEL1-YFP were not overly toxic to cells.

We observed that RTEL1-YFP localization is predominantly diffuse within the nucleus (Figure 13), but it can also be detected as faint diffuse fluorescence in the cytoplasm. In addition, we also occasionally observed cells with a low frequency (~1-3 foci) of distinct RTEL1 foci in interphase (Figure 13). It has been well established that

mouse ES cells have a short G1 phase and a large proportion of cells are in S-phase [105, 106]. These results indicate that RTEL1 localization is predominantly nuclear and diffuse with a subset of cells exhibiting spontaneous nuclear foci, likely in S-phase. This is consistent with previous reports which also observed that RTEL1 localizes to the nucleus [28]. It is possible that RTEL1 may be occasionally recruited to foci during S-phase to resolve recombination intermediates which can form during normal replication.

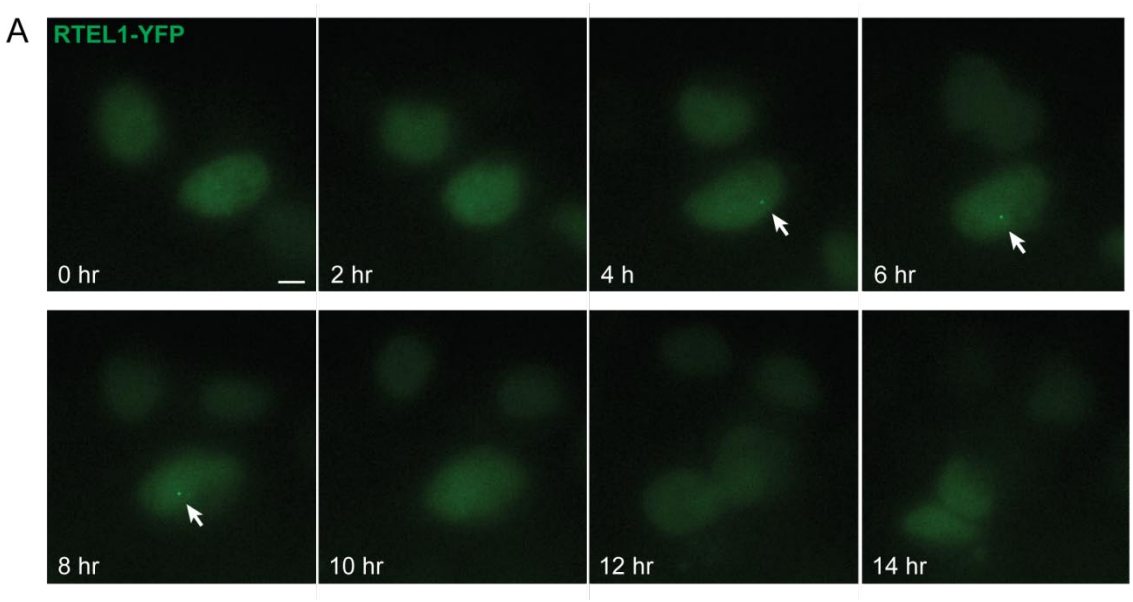

Figure 13. RTEL1 localizes to the nucleus with a subset of cells exhibiting spontaneous nuclear foci in S-phase.

Images from a time-lapse movie showing RTEL1-YFP (green) localization in RTEL1-deficient mouse ES cells. Note that fluorescence is mostly diffuse with a subset of cells exhibiting distinct foci (arrows). Scale bar, 5 μM (Reprinted with permission of ASCB: Mol. Biol.Cell, Uringa, Lisaingo et al. 2012 [1]).

4.2.2 RTEL1 foci formation is induced by DNA damage

We next investigated the cellular localization of RTEL1 in the presence of various DNA damaging agents. Cells expressing RTEL1-YFP were treated with aphidicolin, which blocks DNA synthesis by inhibiting DNA polymerases, or mitomycin C, which induces DNA interstrand crosslinking, and these cells were visualized by live-cell imaging. We observed the formation of RTEL1-YFP foci, which increased in fluorescence intensity and number over time upon treatment with aphidicolin (1 µM) (Figure 14A), or mitomycin C (1 µg/mL for 1 hour prior to imaging) (Figure 14B). The first few faint foci appeared rapidly (~1-6 foci within 2 hrs) and increased considerably in number over time (~20-100 foci at ~20 hrs). The number of RTEL1 foci increased in a dose-dependent manner (data not shown). However, at the concentrations used mitomycin C appeared to induce a higher number of RTEL1 foci than aphidicolin. These results suggest that RTEL1 is recruited to discrete foci in the presence of DNA damage. To our knowledge, this is the first time that RTEL1 has been observed to form distinct foci within the nucleus.

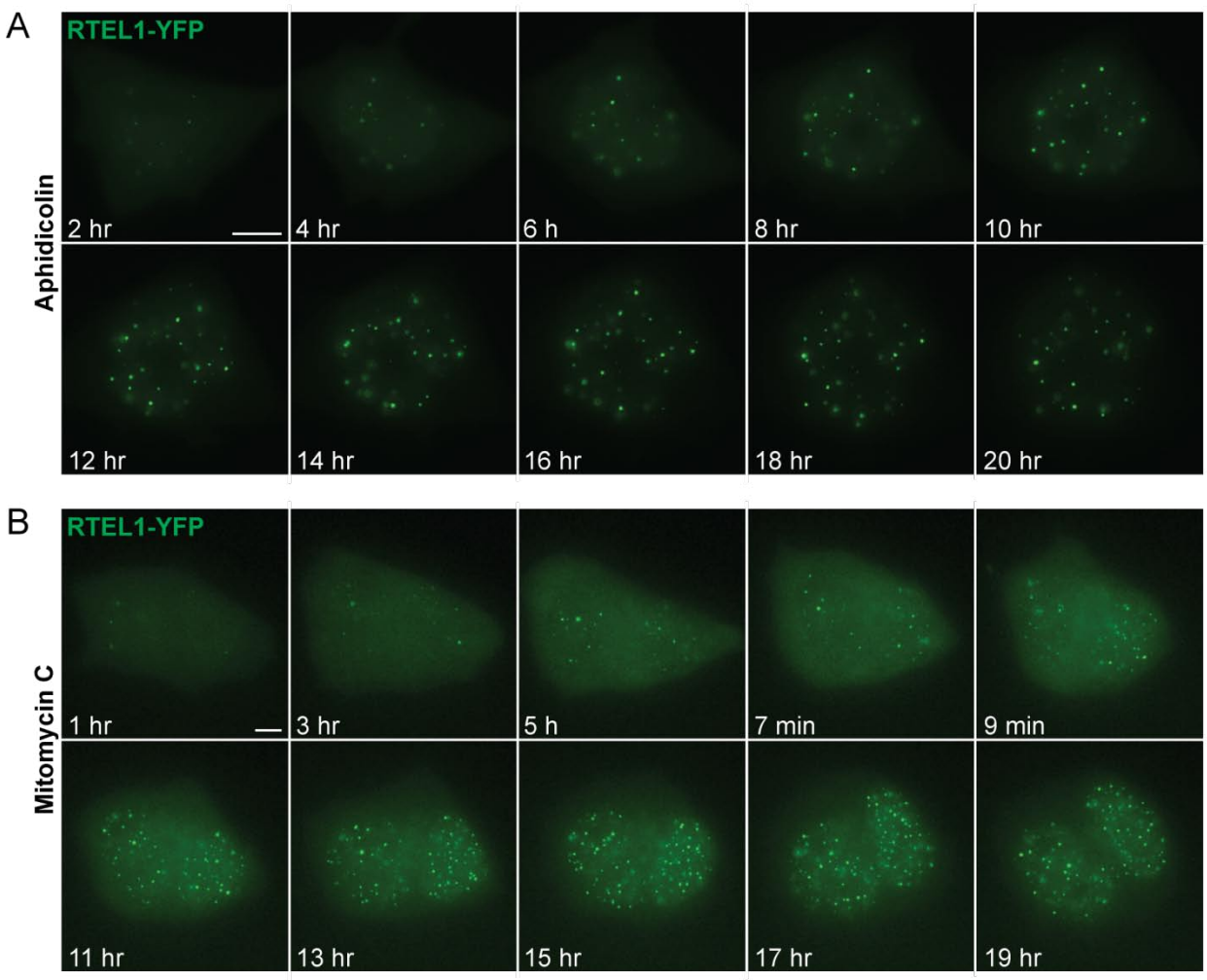

Figure 14. RTEL1 foci formation is induced by DNA damage.

Time-lapse images showing RTEL1-YFP (green) foci formation upon treatment with (A) aphidicolin (1µM) or (B) mitomycin C (1 µg/mL for 1 hour prior to imaging). Note increase in number and intensity of foci over time. Numbers indicate time after addition of DNA damaging agent. Scale bar, 5 µM (Reprinted with permission of ASCB: Mol. Biol.Cell, Uringa, Lisaingo et al. 2012 [1]).

4.2.3 RTEL1 localizes to sites of DNA repair

To determine whether RTEL1 foci form at sites of DNA repair, we assayed for co-localization of RTEL1 with the DNA repair proteins, p53-binding protein 1 (53BP1) and the Fanconi anemia protein FANCD2. 53BP1 is a conserved mediator of the DNA damage checkpoint with properties as an early DNA double-strand break sensor [136, 137]. FANCD2 (Fanconi anemia group D2 protein) is encoded by a gene mutated in Fanconi anemia and is required for chromosome stability and the repair of DNA double-strand breaks [138]. We generated cell lines stably expressing the minimum (M) domain of *53bp1* fused to RFP (RFP-53BP1), where the M domain is the minimum domain required for targeting to DNA double-strand break foci [139]. We next assayed for co-localization of RTEL1 with RFP-53BP1 or a FANCD2 antibody. We find that RTEL1 foci co-localize with almost all 53BP1 and FANCD2 foci in the presence of aphidicolin or mitomycin C (Figure 15 and Movies 12-14). 53BP1 foci were detected before RTEL1 foci, consistent with the role of 53bp1 as an early DNA sensor of DNA breaks [136], however it cannot be excluded that this was a result of differences in fluorescence intensity. Together, these data suggest that in the presence of DNA damage, RTEL1 is recruited to discrete foci at sites of DNA repair.

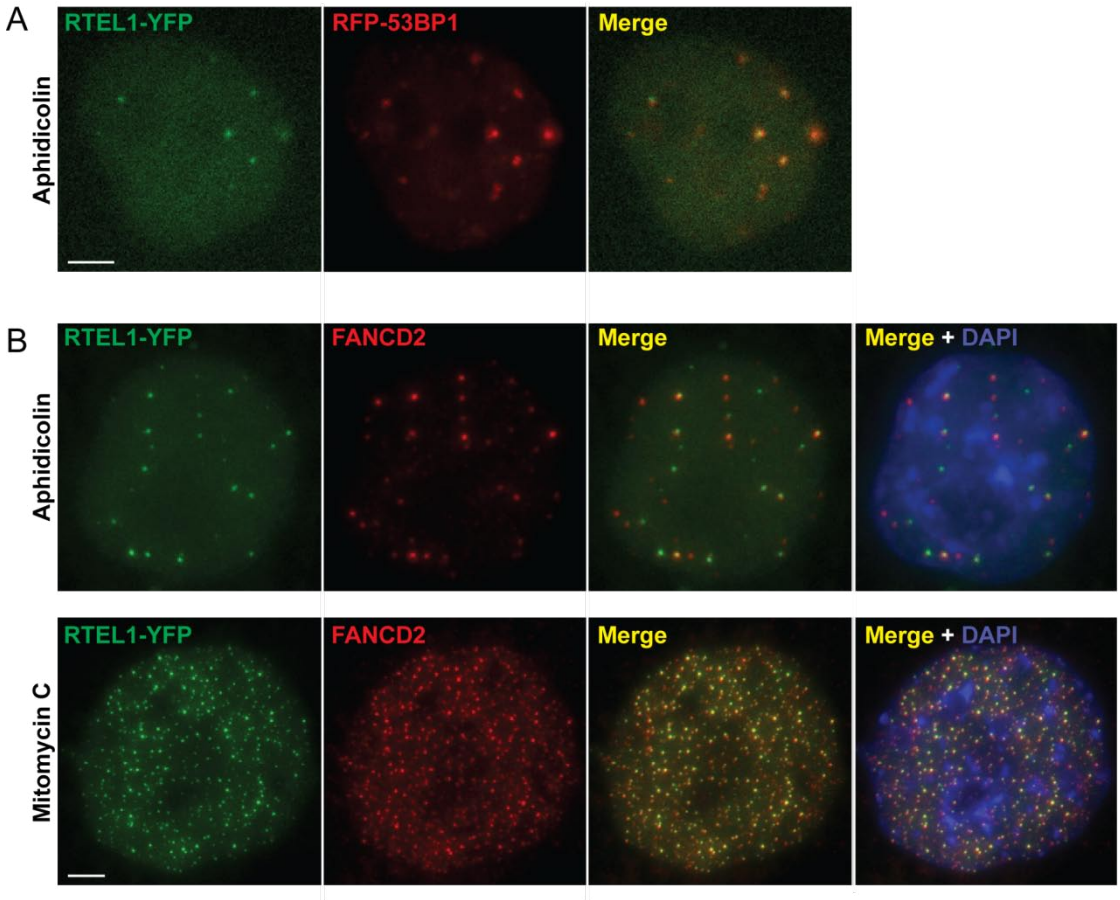

Figure 15. RTEL1 is recruited to sites of DNA damage.

(A) Images showing RTEL1-YFP (green) co-localization with RFP-53BP1 (red) after treatment with aphidicolin (2 µM for 18 hours). Images are of a single z-section. (E) Projection images showing RTEL1-YFP co-localization (yellow) with FANCD2 antibody conjugated to Cy5 (red) after treatment with aphidicolin (1 µM for 24 hours) or mitomycin C (1 µg/mL for 24 hours). DAPI DNA stain (blue). Scale bar, 5 µM (Reprinted with permission of ASCB: Mol. Biol.Cell, Uringa, Lisaingo et al. 2012 [1]).

Movie 12. RTEL1 co-localizes with 53BP1 at sites of DNA damage (RFP).

Movie 13. RTEL1 co-localizes with 53BP1 at sites of DNA damage (YFP).

Movie 14. RTEL1 co-localizes with 53BP1 at sites of DNA damage (Merge).

Live-cell fluorescence imaging of mouse ES cells expressing RTEL1-YFP (green) and RFP-53BP1 (red) upon treatment with aphidicolin (1 μM). Scale bar, 5 μM (Re-displayed with permission of ASCB: Mol. Biol.Cell, Uringa, Lisaingo et al. 2012 [1]). See attached CD for movies.

4.2.4 Localization of RTEL1 to persistent TRF1 bridges at telomeres

Since RTEL1 was proposed to be recruited by TRF1 to telomeres [93], we sought to determine whether RTEL1 would be recruited to the telomere associations and segregation defects induced by TRF1 overexpression observed in Chapter 2. Cells stably expressing RTEL1-YFP were transiently transfected with RFP-TRF1, sorted for RFP-positive cells using FACS to obtain a bulk population of cells with various levels of TRF1 expression, and these cells were imaged at 48 to 72 hours post-transfection.

We observed a striking phenotype whereby distinct RTEL1 foci localized to the extremities of persistent TRF1 bridges (Figure 16A). In addition, a thin thread of RTEL1 was often observed that co-localized with TRF1 bridges and connected these flanking RTEL1 foci. RTEL1 foci were observed predominantly at TRF1 bridges between daughter cells with decondensed chromosomes, suggesting that cells were in the later stages of mitosis or interphase. Intriguingly, formation of distinct RTEL1-YFP foci appeared to be restricted to persistent TRF1 bridges, and did not co-localize with non-bridge RFP-TRF1 foci throughout the rest of the cell (Figure 16A). These results suggest that RTEL1 is recruited specifically to persistent TRF1 bridges, possibly to

resolve TRF1-mediated telomere associations. To our knowledge, this is the first evidence of RTEL1 cellular localization to telomeres.

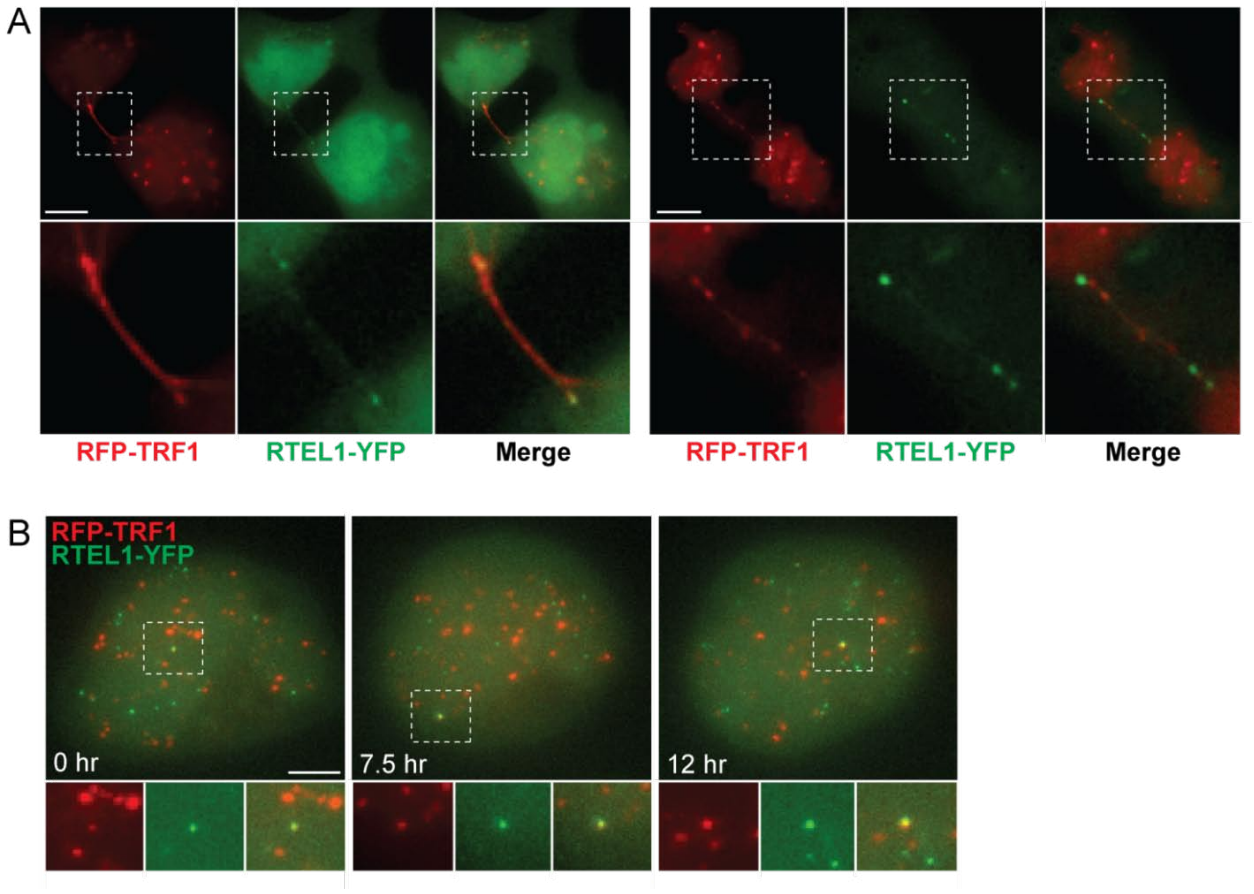

Figure 16. Localization of RTEL1 to persistent TRF1 bridges at telomeres.

(A) Images showing localization of RTEL1-YFP (green) to distinct foci at the extremities of persistent RFP-TRF1 bridges (red). A thin thread of RTEL1-YFP can also be observed along the length of the bridge, connecting these foci. (B) Time-lapse images showing co-localization (insets) of some but not all RFP-TRF1 and RTEL1-YFP foci. Three different timepoints from a movie of the same cell are shown. Scale bar, 5 µM (Figure 16B was reprinted with permission of ASCB: Mol. Biol.Cell, Uringa, Lisaingo et al. 2012 [1]).

It is not clear whether RTEL1 was also recruited to TRF1 bridges at an earlier stage in mitosis, since RTEL1 localization was diffuse for the duration of mitosis. RTEL1 foci present prior to mitosis, induced by aphidicolin, mitomycin C or TRF1 overexpression, appeared to dissociate upon entry into mitosis, and foci often reappeared as cells exited mitosis and chromosomes decondensed (data not shown).

RTEL1 foci formation was also observed in interphase cells upon TRF1 overexpression, where certain cells exhibited a low degree of co-localization between TRF1 and RTEL1. Figure 16B shows three timepoints from a movie of the same cell, in which overlapping RTEL1-YFP and RFP-TRF1 foci are observed. Although visually there was an overall increase in RTEL1 foci upon TRF1 overexpression, we did not observe a clear trend between the intensity or size of RFP-TRF1 foci and co-localization with RTEL1-YFP foci in interphase cells (Figure 16B).

Taken together, these results suggest that RTEL1 is specifically recruited to persistent TRF1 bridges at telomeres, and is transiently recruited to a subset of telomeres in interphase.

4.3 Discussion

We predicted that the essential helicase RTEL1 might be recruited to resolve or repair the telomere associations and segregation defects observed in chapter 2. We uncovered a striking phenotype where RTEL1 formed distinct foci which localized

specifically to the extremities of TRF1 bridges. A thin thread of RTEL1 was also observed along the TRF1 bridge. Since RTEL1 appeared to localize specifically to TRF1 bridges, this suggests that the co-localization of TRF1 and RTEL1 is not due to random probability. Our results support the hypothesis that RTEL1 is recruited to telomeres, possibly to resolve TRF1-mediated telomere associations.

We also observed that RTEL1 forms discrete foci upon treatment with DNA damaging agents, which co-localize with almost all 53BP1 and FANCD2 foci, suggesting that RTEL1 is recruited to sites of DNA repair. Mitomycin C induced an overall higher incidence of RTEL1 foci compared to aphidicolin at the concentrations used, suggesting that DNA interstrand crosslinking is a potent inducer of RTEL1 foci formation.

Other studies have shown similar localization of certain Fanconi anemia proteins to ultra-fine bridges containing the helicases BLM (the causative gene of Bloom Syndrome) and PICH (PLK-interacting checkpoint helicase) [140]. FANCD2 was observed at the extremities of ultra-fine bridges [140], and FANCM was recruited to ultra-fine bridges specifically at a later stage in mitosis [141]. Ultra-fine bridges have been observed at centromeres and fragile-sites but ultra-fine bridges at telomeres are not well characterized, and FANCD2 was only rarely observed at regions close to, but not co-localizing with, telomeres [140]. Further studies will likely reveal how telomere bridges containing TRF1 and RTEL1 compare to ultra-fine bridges.

4.3.1 Model for RTEL1 function

We observed recruitment of RTEL1 to TRF1 bridges at telomeres and sites of DNA repair, suggesting that RTEL1 may have a similar function at both these sites. *In vitro* studies have shown that RTEL1 resolves a specific structure called a D loop (displacement loop) [89]. D loops form by invasion of a 3' ssDNA overhang into dsDNA [89]. D loops are thought to form during DNA repair by homologous recombination, following resection of DNA double-strand breaks to generate 3' ssDNA overhangs. However, similar structures might also form at telomeres when the 3' ssDNA overhang at the extreme telomere end invades duplex telomeric DNA. D loops can form at telomeres by two mechanisms: by folding back on itself to form the T loop, or during telomere strand exchange between different telomeres (Figure 17). RTEL1 has been proposed to resolve D loops at telomeres by promoting displacement of the invading strand (for review [2]) (Figure 17).

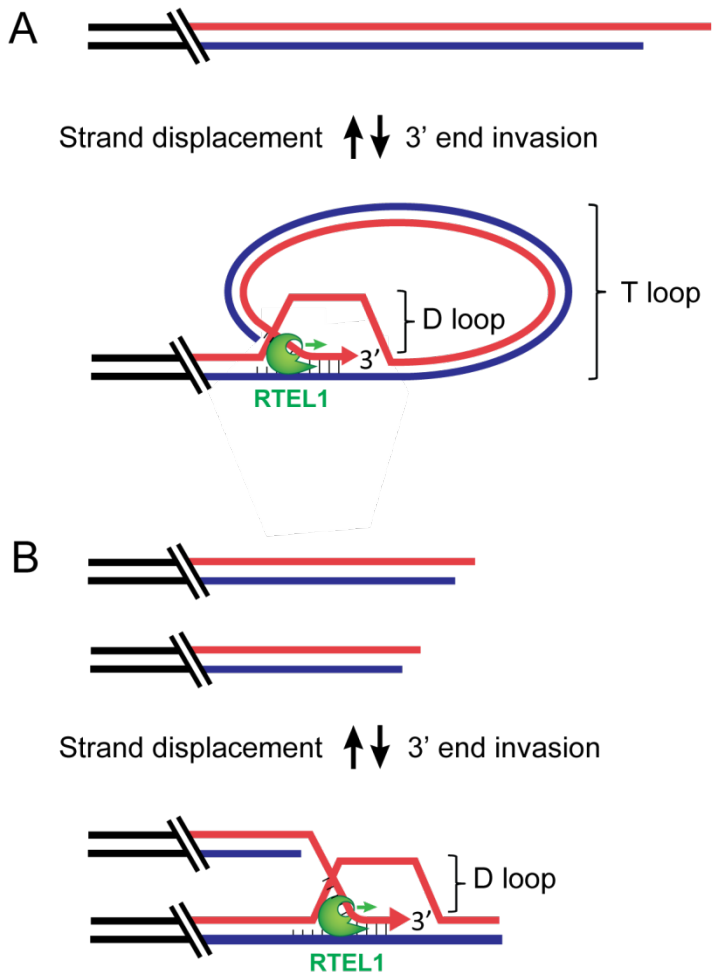

Figure 17. Model for RTEL1 function at telomeres.

RTEL1 (green) resolves D loops, which form by invasion of a 3’ ssDNA overhang into dsDNA. D loops may form at telomeres (A) by folding back on itself to form the T loop, or (B) during telomere strand exchange between different telomeres. RTEL1 promotes strand displacement at D loops, possibly by associating with the ssDNA-dsDNA junction via an iron sulphur domain and translocating in the 5' to 3' direction [2, 89] (Reprinted with permission of Oxford Journals: Nucleic Acids Res., Uringa et al. 2010 [2]).

We observed that RTEL1 is specifically recruited to persistent TRF1 bridges. These persistent bridges may represent a subset of telomere associations that have progressed into DNA-mediated interactions. It is tempting to speculate that TRF1-mediated telomere associations that are not resolved in a timely manner may undergo telomere strand exchange, leading to the recruitment of RTEL1 to resolve telomeres by promoting strand displacement.

Chapter 5: Experimental methods

5.1 Plasmid constructs

Fluorescent TRF1 and H2B was generated by fusion to fluorescent proteins as specified in the text. The fluorescent proteins used throughout this study were Venus yellow fluorescent protein (YFP) [115], mCherry red fluorescent protein (RFP) [122], and Cerulean cyan fluorescent protein (CFP) [135]. For the IRES-YFP control vector and $TRF1_{IRES\text{-}YFP}$ constructs an IRES-domain was fused to the N-terminus of YFP and a fragment containing the N-terminus of nuclear membrane-localizing domain, importin alpha1 fragment. The FKBP12-L106P mutant [134] was fused to the N-terminus of YFP-$TRF1_{TEV}$ or the C-terminus of RTEL1-YFP. Expression of all constructs was driven by a CAG (CMV early enhancer/chicken beta-actin) promoter, except for RTEL1-YFP which was driven by a PGK (phophoglycerate kinase) promoter, and CFP-TEV protease which was driven by a CAG or a PGK promoter as specified.

5.2 Cell culture and plasmid transfection

Mouse ES cell lines (129 strain) were grown under standard culture conditions on 0.1% gelatin-coated dishes in the presence of leukemia inhibitory factor, as described previously [142]. Cell transfection was performed using Qiagen effectene transfection reagent (Mississauga, Ontario) to obtain transient or stably expressing cell lines as specified. The RTEL1-deficient cell lines used in this study was previously generated by intercrossing *Rtel1* +/- mice (129S1) and establishing mouse ES cell lines [28].

5.3 FACS analysis

Cell populations expressing defined TRF1 protein levels were obtained by transiently transfecting mouse ES cells with the YFP-TRF1, $TRF1_{IRES\text{-}YFP}$, or YFP-$TRF1_{TEV}$, as specified in the text. Cells were sorted by FACS (BD Influx, Becton Dickinson, Cytopeia) and data was analyzed using FlowJo software (Treestar).

5.4 Preparation of whole cell extracts and Western blotting

Whole cell extracts were prepared by growing mouse ES cells, transiently expressing $TRF1_{IRES\text{-}YFP}$ or YFP-TRF1 and sorted for low, medium, or high YFP levels, to ~80% confluence in 15cm dishes. At 48 hours post-transfection, cells were harvested by trypsinization, counted, pelleted and incubated at 4^{o}C in NuPAGE LDS-reducing sample buffer (Invitrogen). Cells were stored at -20^{o}C until use in western blotting assay.

Proteins from whole cell extracts were heated to 70^{o}C for 10min before separation by standard SDS-PAGE (XCell SureLock system; 10% NuPAGE Bis-Tris gel in MOPS running buffer; Invitrogen). Following transfer to a nitrocellulose membrane (Bio-Rad), membrane strips were blocked (5% nonfat dry milk, 5% BSA, and 0.1%Tween 20 in TBS [TBS-MTB]) for 1 h, and incubated overnight with the following antibodies, rabbit anti-mouse TRF1 (1:1000 in TBS-MTB; TRF12-S; Alpha Diagnostic), anti-GFP (1:50000 in TBS-MTB; Ab290; Abcam) or GAPDH (Research Diagnostics Inc) as a loading control. Proteins were visualized by chemiluminescence (SuperSignal West Pico; Thermo Scientific Pierce).

5.5 Immunostaining and FACS analysis for counting TRF1 foci

A cell clone stably expressing low levels of YFP-TRF1 was generated and these cells were fixed in suspension with 4% formaldehyde in PBS for 20min, permeabilized in 0.2% NP-40 in PBS, blocked with 1% bovine serum albumin in PBS, incubated with a rabbit anti-phospho-histone H3 (Ser10) (06-570; Upstate) mitotic marker conjugated to goat anti-rabbit Cy5 (111-175-003; Jackson Immunoresearch), and stained with DAPI (4',6-diamidino-2-phenylindole). These cells were sorted, using a BD Influx cell sorter (Becton Dickinson Cytopeia), based DAPI DNA content into G1, S, and G2/M directly onto pre-cleaned slides and mounted in antifade containing 2.3% 1,4-diazabicyclo[2.2.2]octane (DABCO, Sigma). Image stacks of whole cells were acquired for 20 cells from each sorted cell population (z-section spacing 0.2 µm). Deconvolved images were analyzed using Volocity (Improvision, Perkin Elmer), where cells were selected using automatic thresholding of fluorescence intensity.

5.6 Time-lapse fluorescence microscopy

Mouse ES cells were grown in #1.5 Labtek II chambered coverglasses (Nalge NUNC, Rochester, NY) coated with gelatin. In order to adhere gelatin to the glass, the glass was coated with 0.1% gelatin, air dried, fixed with 4% paraformaldehyde for 2 hours, and rinsed thoroughly with PBS. Cells grown using this method had normal morphology compared to standard gelatin-coated plastic dishes. Time-lapse microscopy was performed using a Deltavision RT system (Applied Precision) with an Olympus IX inverted microscope and a CoolSnap HQ CCD camera (Roper Scientific). The following

excitation and emission filters were used: CFP: 436/10 and 465/30 nm, YFP: 492/18 and 535/30 nm, and RFP: 580/20 and 630/60 nm. Images were acquired using a 60x PlanApo 1.4 NA oil objective (Olympus). Cells were maintained in an environmental chamber at 37^{o}C with 5% CO_2 perfusion. Images were analyzed using SoftWoRx Suite software (Applied Precision) and Volocity (Improvision, Perkin Elmer).

Cells were imaged starting in metaphase for TRF1 bridge assay, where image stacks (15 images, z-section spacing: 1 µM) were acquired at 5 min intervals. Exposure was 0.2 seconds and neutral density filters (transmission 10%) were used to minimize photobleaching effects.

5.7 Metaphase spread preparation and telomere FISH

Sorted cell populations of mouse ES cells expressing low, medium or high levels of IRES-YFP, $TRF1_{IRES\text{-}YFP}$, or YFP-TRF1 were treated with colcemid (0.1 µg/ml) for 4 hours prior to harvesting cells with trypsin. After washing and hypotonic swelling (75mM KCl) for 3 to 5 min at 37^{o}C, cells were fixed twice in methanol-acetic acid (3:1) at RT for 15 min. One drop of cell suspension was spread onto a pre-cleaned slide, and air-dried overnight. Telomere FISH was performed as previously described [143] using a Cy5-conjugated $(C_3TA_2)_3$ peptide nucleic acid probe (Boston Probes, Applied Biosystems). Images were acquired on a Zeiss Axioplan 2 microscope (Carl Zeiss) equipped with Isis 5 software (Metasystems) using a Axiocam MRm camera (Carl Zeiss).

5.8 TRF1 cleavage assay

The same automatic thresholding of fluorescence intensity was used for all timepoints. Timepoints were selected at which the entire cell was in focus, and ranged from 1-10 hours before and after detection of CFP-TEV Protease. TEV Protease was fused to nuclear localization signals at the N- and C-terminus (CFP-NLS-TEV protease-NLS-NLS), which has been reported to facilitate nuclear entry of TEV protease [130]. The TEV protease recognition site ENLYFQGx3 was inserted in the flexible hinge region of *mTrf1* using similar methods to Pauli et al. 2008 [130]. An HpaI site was introduced into TRF1 at amino acid position 338 by site-directed mutagenesis using the oligonucleotide 5'-GAAACAACGATGGAAGTTAACCGAAGAACC-3'. The TEV protease recognition site ENLYFQGx3 was then inserted at the HpaI site using the oligonucleotide 5'-PHOSPHATE-AACGCTCTAGAGAAT TTGTATTTTCAGGGTGCTTCTGAAAACCT TTACTTCCAAGGAGAGCTCGAAAATCTTTATTTCCAGGGAGTT-3'.

Chapter 6: Discussion

6.1 Summary of findings

In chapter 2, we described the development of a system for high resolution visualization of telomere and chromosome dynamics using multicolor live-cell fluorescence imaging. Using this system, cells expressing defined levels of TRF1 protein were examined and it was found that TRF1 overexpression induces TRF1 bridging in anaphase, TRF1 aggregates and mitotic bypass. Analysis of telomeric DNA distribution in metaphase chromosomes, revealed two forms of telomere associations: single or joined sister telomeres, as well as telomere aggregates between multiple chromosomes. These results support the concept that precise regulation of cellular TRF1 levels is essential for telomere resolution and mitotic progression.

In chapter 3, we described the development of a novel assay that combines site-specific protein cleavage of TRF1 by TEV protease with live-cell fluorescence imaging in a mammalian system. We observed that the cellular localization of fluorescent cleavable TRF1 changed from distinct foci to a diffuse fluorescence, at the same time as detection of nuclear TEV protease, suggesting that TRF1 was successfully cleaved. This system was used to directly test a potential mechanism for TRF1-mediated telomere cohesion. We observed that telomere aggregates induced by TRF1 overexpression are resolved upon TEV protease-mediated TRF1 cleavage, suggesting that telomere associations result primarily from TRF1-mediated protein interactions. Further validation of these results is required.

In chapter 4, we characterized the cellular localization of RTEL1 in the presence of telomere dysfunction and DNA damage. We uncovered a striking phenotype where RTEL1 formed distinct foci which localized specifically to the extremities of TRF1 bridges. In the presence of DNA damage, RTEL1 formed distinct foci which co-localized with DNA damage response proteins, suggesting that RTEL1 is recruited to sites of DNA repair. A model linking RTEL1 function at telomeres and sites of DNA repair was presented, where RTEL1 might promote strand displacement during telomere strand exchange between associated telomeres or during DNA repair by homologous recombination. To our knowledge, this is the first time that RTEL1 has been observed to form distinct foci within the nucleus, and the first evidence of RTEL1 cellular localization to telomeres.

6.2 Overall analysis and significance

Telomere associations could play key roles under physiological conditions, such as during meiosis, from replication until mitosis, or during telomere recombination and repair events. In a nearly universal mechanism, telomere clustering occurs during telomere bouquet formation in meiosis, which might facilitate the alignment of homologous chromosomes prior to their recombination and segregation. Intriguingly, Taz1 (the TRF1/TRF2 ortholog in *S.pombe*) is required to stabilize telomere associations during this process [81]. Based on observations of telomere associations in mitosis of tankyrase 1-depleted cells, a mechanism for telomere cohesion was

described [78, 87], which may function to hold sister-telomeres together from replication until mitosis, in a similar manner to cohesins at centromeres and along chromosome arms. Telomere cohesion has been proposed to serve as a distinct checkpoint at the chromosome end, which may allow cells to monitor the intactness of the chromosome prior to cell division [87]. This checkpoint may ensure that sister telomeres are fully replicated, paired and intact, and may be activated during replication fork stalling or when chromosome breaks lead to loss of the telomere. Telomere associations that persist over time could promote to telomere strand invasion, which may facilitate telomere repair by homologous recombination, or lead to the recruitment of strand displacing helicases such as RTEL1 to resolve these structures.

Telomere associations could also play key roles under pathological conditions. Telomere aggregates, as well as TRF1 overexpression and depletion have been observed in human cancer [82, 144-149]. If telomere associations form preferentially when the ratio of telomere repeats is limiting compared to TRF1 protein levels, then as telomeres shorten and the relative concentration of TRF1 per telomere repeats increases (assuming that TRF1 expression levels remain relatively constant), TRF1-mediated telomere associations might form. This suggests a potential mechanism for the telomere aggregates observed in cancer cells (Figure 18).

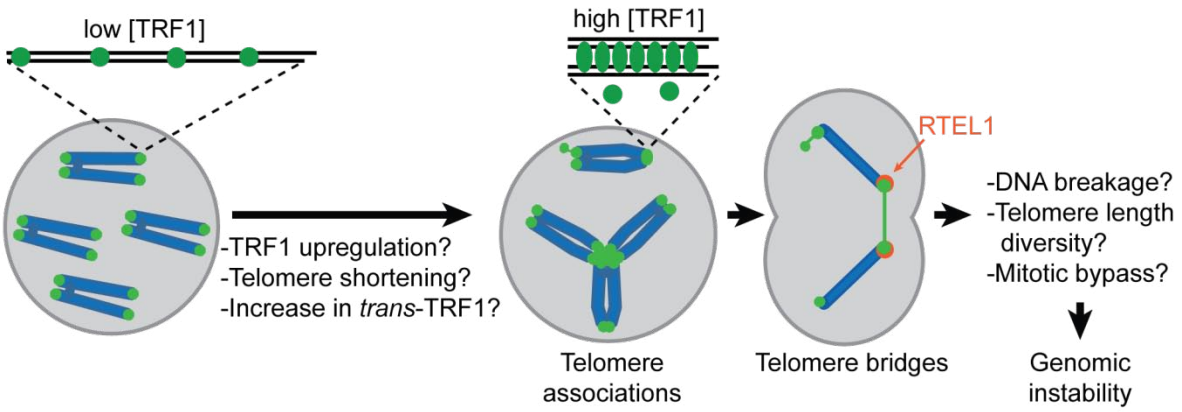

Figure 18. Model for TRF1-mediated telomere associations.

If telomere associations form preferentially when the ratio of telomere repeats is limiting compared to TRF1 protein levels, then telomere associations can occur by an increase in TRF1 levels, a decrease in telomere length, or under conditions which promote the *trans*-TRF1 conformation. Telomeres that are not resolved prior to mitosis, may lead to telomere bridges which recruit RTEL1 to resolve telomere associations. Telomere bridges may lead to chromatin breaks that continue to fuse and break in subsequent cell cycles, giving rise to genomic instability.

The tumour suppressor gene p53 is essential for maintaining genomic stability and is mutated in the majority of human cancers [150]. We find that mouse ES cells, which divide rapidly and lack a functional p53 checkpoint [105, 113], progress through mitosis in the presence of telomere dysfunction, giving rise to anaphase bridges at telomeres, mitotic bypass and tetraploidization. This is consistent with studies showing that persistent telomere dysfunction in p53-deficient cells leads to tetraploidization and mitotic bypass [123]. Therefore, deregulation of TRF1 levels could lead to more severe chromosome instability phenotypes in cells without p53 checkpoints, such as cancer

cells, than in cells with intact p53 checkpoints. Telomeres that are not resolved prior to mitosis can lead to anaphase bridges at telomeres and chromatin breaks, which continue to fuse and break in subsequent cell cycles, giving rise to genomic instability (Figure 18). If chromatin bridges were to predominantly break at telomeric DNA, telomere associations could contribute to the heterogeneity in telomere length at any given telomere [26].

6.3 Strengths and limitations

By combining the TRF1 cleavage assay with live-cell imaging, we had the advantage of visualizing telomere dynamics upon TRF1 cleavage in real-time. Although the TRF1 cleavage assay can be used to show how cleavage of TRF1 protein affects resolution of telomere aggregates, our studies alone cannot exclude additional contributing factors, such as the conformation of TRF1, TRF1 multimerization with other TRF1 dimers, or the effect of other proteins at telomeres.

Several studies argue against the possibility that telomere associations are due to TRF1 multimerization with other TRF1 dimers. Individual TRF1 dimers have not been shown to interact with each other with significant affinity [42, 55], and a single TRF1 dimer appeared to be sufficient to induce telomeric DNA looping [4]. However, it cannot be excluded that TRF1 may undergo multimerization at high protein levels and further studies are required. It also cannot be excluded that two TRF1 dimers in *cis* on opposing telomere strands could be bridged by other proteins. However, it is unlikely

that proteins bridging TRF1 dimers would lead to increased telomere aggregation upon TRF1 overexpression, due to limiting numbers of these proteins in comparison to TRF1.

It is likely that other proteins within and outside the shelterin complex also regulate the degree to which telomeres associate at different stages of the cell cycle in different cell types. TRF1 forms a complex with other proteins implicated in telomere associations, such as TIN2 and the cohesin subunit SA1 [80] [48]. Although TRF1 alone is sufficient to stimulate clustering of telomeric DNA tracts *in vitro*, addition of TIN2 stimulates an increase in telomere clustering activity by fivefold to tenfold [55, 86], suggesting that TIN2 facilitates TRF1-mediated telomere associations. Different forms of cohesin have been described in vertebrates, with varying subunit compositions. Telomere-specific cohesins usually contain the subunit SA1, whereas centromere-specific cohesins usually contain the subunit SA2 [151]. TRF1 has been suggested to recruit telomere-specific cohesin complexes to telomeres by binding to SA1 but only a small fraction of endogenous TRF1 associates with SA1 [80]. Both TRF1 and SA1 are required for efficient replication of telomeres and depletion of both these proteins leads to fragile-telomere phenotypes, such as multiple or elongated telomeric-FISH signals [79, 93, 94, 152]. This suggests that dual roles exist for TRF1 and SA1 in telomere cohesion and replication. Indeed, an important step during replication is the establishment of cohesion between sister chromatids, which prevents premature separation of sister-chromatids [153], suggesting that cohesion is required for efficient replication. Several questions remain: Does TRF1 protein itself mediate telomere associations *in* vivo, as it has been shown to do *in vitro*? How do other proteins, within

and outside the shelterin complex, regulate telomere associations? Or does TRF1 induce telomere associations indirectly by recruiting telomere-specific cohesion complexes to telomeres? Further studies are needed to distinguish between these possibilities.

It cannot be excluded that high levels of TRF1 binding to telomeres may occupy available telomere-binding sites, leading to displacement of other telomere-binding proteins such as TRF2. TRF1 has been shown to bind telomeres 4x more strongly than TRF2 [154]. The TRF2-depletion phenotype consists of chromosome end-to-end fusions characteristic of telomere uncapping or telomere shortening [63]. Although we occasionally observed metaphase chromosomes positioned end-to-end, the predominant phenotype in TRF1- overexpressing cells was sister-telomere associations and telomere aggregates involving several different chromosomes positioned radially, suggesting that the TRF1 overexpression phenotype is mostly distinct from the TRF2-depletion phenotype. Future studies could involve a close comparison of the phenotypes induced by deregulation of TRF1 and TRF2.

Our results suggest that telomere associations are mediated primarily by protein interactions as opposed to DNA interactions, since cleavage of TRF1 protein resolved telomere aggregates. However, we occasionally observed telomere aggregates that remained after detection of TEV protease. It is not clear whether these remaining telomere aggregates represented TRF1-mediated protein interactions that could not be cleaved by TEV protease, or another type of interaction. DNA-mediated interactions can

arise via processes such as recombination, telomere fusion, stalled telomere replication or DNA catenation. It is possible that telomeres that are initially associated via protein-mediated interactions could eventually progress into DNA-mediated interactions. This is supported by studies showing that persistent sister-telomere associations in tankyrase 1-deficient cells, which may be initially associated by protein interactions, progress into telomere DNA fusions by NHEJ within 48 hours after tankyrase 1 knockdown [155].

6.4 Potential applications and possible future research

Future studies currently being explored in the Lansdorp lab include using cells that undergo mitotic arrest in the presence of unresolved telomeres, similar to the mitotic arrest observed in the tankyrase 1-depleted HeLa immortalized human tumor cell line [78]. We propose that TRF1 cleavage will lead to resolution of telomeres, release from mitotic arrest and chromosome segregation. We are also currently conducting studies in which cells expressing defined levels of a construct encoding cleavable TRF1 translated separately from the fluorescent fusion tag are fixed before and after detection of TEV-protease, and assayed for resolution of telomeres using telomere-FISH probes. We have also generated constructs for inducible expression of CFP-TEV protease using a Cre-Lox system, which should facilitate expression of TEV protease in a more controlled manner than transient transfection.

Our studies using cleavage of the unstructured TRF1 flexible linker could be complemented with studies examining how disruption of other sites within TRF1 affects telomere associations. It is likely that the TRF1 dimerization domain is required for

telomere associations. However, TEV protease-mediated cleavage of the TRF1 dimerization domain might be difficult since there are a number of hydrophobic interactions along the dimerization interface [59] and the TEV protease recognition site might not be easily accessible to TEV protease. An alternative method is to introduce mutations in the dimerization domain. Other studies have shown that certain TRF1 homodimerization mutants can still bind and localize to telomeres, albeit with a decreased telomere-binding affinity compared to wild-type TRF1 [59]. Consequently, these experiments may be limited by the inability to distinguish whether an absence of telomere associations is a result of mutations in the dimerization domain or a decreased TRF1-binding affinity to telomeres. Furthermore, competition assays with TRF1 dimerization mutants may be limited by the amount of mutated TRF1 required to efficiently compete out the high levels of exogenous TRF1.

Future studies could involve high resolution imaging of chromatin structure. For instance, transmission electron microscopy could be used to examine chromatin preparations from cells overexpressing TRF1. These studies could provide further insight into how TRF1 mediates telomere associations in a cellular context, in comparison to previous electron microscopy studies using TRF1 protein and DNA tracts in isolation.

6.5 Concluding remarks

Telomere associations have been observed during key cellular processes, including mitosis, meiosis, and cancer. Previous studies have begun to elucidate the

mechanism of telomere associations, and have implicated a role for TRF1. Our studies provide support for TRF1-mediated telomere associations in a cellular context. Future studies will likely further reveal how this mechanism is mediated, what other factors within and outside the shelterin complex might play a role, and how telomere associations affect cellular processes under physiological and pathological conditions.

References

1. Uringa, E.J., et al., *RTEL1 contributes to DNA replication, repair and telomere maintenance.* Molecular biology of the cell, 2012.
2. Uringa, E.J., et al., *RTEL1: an essential helicase for telomere maintenance and the regulation of homologous recombination.* Nucleic Acids Res, 2010.
3. Denchi, E.L., *Give me a break: how telomeres suppress the DNA damage response.* DNA Repair (Amst), 2009. **8**(9): p. 1118-26.
4. Bianchi, A., et al., *TRF1 binds a bipartite telomeric site with extreme spatial flexibility.* The EMBO journal, 1999. **18**(20): p. 5735-44.
5. Blackburn, E.H., *Structure and function of telomeres.* Nature, 1991. **350**(6319): p. 569-73.
6. Muller, H.J., *The remaking of chromosomes.* Collecting Net, 1938. **8**: p. 182-195, 198.
7. McClintock, B., *The stability of broken ends of chromosomes in Zea mays.* Genetics, 1941. **26**: p. 234-282.
8. de Lange, T., *How telomeres solve the end-protection problem.* Science, 2009. **326**(5955): p. 948-52.
9. Watson, J.D., *Origin of concatemeric T7 DNA.* Nat New Biol, 1972. **239**(94): p. 197-201.
10. Olovnikov, A.M., *A theory of marginotomy. The incomplete copying of template margin in enzymic synthesis of polynucleotides and biological significance of the phenomenon.* J Theor Biol, 1973. **41**(1): p. 181-90.
11. Lingner, J., J.P. Cooper, and T.R. Cech, *Telomerase and DNA end replication: no longer a lagging strand problem?* Science, 1995. **269**(5230): p. 1533-4.
12. Klobutcher, L.A., et al., *All gene-sized DNA molecules in four species of hypotrichs have the same terminal sequence and an unusual 3' terminus.* Proc Natl Acad Sci U S A, 1981. **78**(5): p. 3015-9.
13. Henderson, E.R. and E.H. Blackburn, *An overhanging 3' terminus is a conserved feature of telomeres.* Mol Cell Biol, 1989. **9**(1): p. 345-8.
14. Harley, C.B., A.B. Futcher, and C.W. Greider, *Telomeres shorten during ageing of human fibroblasts.* Nature, 1990. **345**(6274): p. 458-60.
15. Lansdorp, P.M., *Repair of telomeric DNA prior to replicative senescence.* Mech Ageing Dev, 2000. **118**(1-2): p. 23-34.
16. Sfeir, A.J., et al., *Telomere-end processing the terminal nucleotides of human chromosomes.* Mol Cell, 2005. **18**(1): p. 131-8.
17. Makarov, V.L., Y. Hirose, and J.P. Langmore, *Long G tails at both ends of human chromosomes suggest a C strand degradation mechanism for telomere shortening.* Cell, 1997. **88**(5): p. 657-66.
18. Wellinger, R.J., et al., *Evidence for a new step in telomere maintenance.* Cell, 1996. **85**(3): p. 423-33.
19. Henle, E.S., et al., *Sequence-specific DNA cleavage by Fe2+-mediated fenton reactions has possible biological implications.* J Biol Chem, 1999. **274**(2): p. 962-71.
20. Oikawa, S. and S. Kawanishi, *Site-specific DNA damage at GGG sequence by oxidative stress may accelerate telomere shortening.* FEBS Lett, 1999. **453**(3): p. 365-8.
21. Lansdorp, P.M., *Major cutbacks at chromosome ends.* Trends Biochem Sci, 2005. **30**(7): p. 388-95.
22. d'Adda di Fagagna, F., et al., *A DNA damage checkpoint response in telomere-initiated senescence.* Nature, 2003. **426**(6963): p. 194-8.
23. Greider, C.W. and E.H. Blackburn, *Identification of a specific telomere terminal transferase activity in Tetrahymena extracts.* Cell, 1985. **43**(2 Pt 1): p. 405-13.

24. Cohen, S.B., et al., *Protein composition of catalytically active human telomerase from immortal cells.* Science, 2007. **315**(5820): p. 1850-3.
25. Allshire, R.C., M. Dempster, and N.D. Hastie, *Human telomeres contain at least three types of G-rich repeat distributed non-randomly.* Nucleic Acids Res, 1989. **17**(12): p. 4611-27.
26. Martens, U.M., et al., *Short telomeres on human chromosome 17p.* Nat Genet, 1998. **18**(1): p. 76-80.
27. Kipling, D. and H.J. Cooke, *Hypervariable ultra-long telomeres in mice.* Nature, 1990. **347**(6291): p. 400-2.
28. Ding, H., et al., *Regulation of murine telomere length by Rtel: an essential gene encoding a helicase-like protein.* Cell, 2004. **117**(7): p. 873-86.
29. Flores, I., et al., *The longest telomeres: a general signature of adult stem cell compartments.* Genes Dev, 2008. **22**(5): p. 654-67.
30. Aubert, G. and P.M. Lansdorp, *Telomeres and aging.* Physiol Rev, 2008. **88**(2): p. 557-79.
31. Hiyama, E. and K. Hiyama, *Telomere and telomerase in stem cells.* Br J Cancer, 2007. **96**(7): p. 1020-4.
32. Shay, J.W. and W.E. Wright, *Senescence and immortalization: role of telomeres and telomerase.* Carcinogenesis, 2005. **26**(5): p. 867-74.
33. Hanahan, D. and R.A. Weinberg, *Hallmarks of cancer: the next generation.* Cell, 2011. **144**(5): p. 646-74.
34. Cesare, A.J. and J.D. Griffith, *Telomeric DNA in ALT cells is characterized by free telomeric circles and heterogeneous t-loops.* Mol Cell Biol, 2004. **24**(22): p. 9948-57.
35. Griffith, J.D., et al., *Mammalian telomeres end in a large duplex loop.* Cell, 1999. **97**(4): p. 503-14.
36. Nikitina, T. and C.L. Woodcock, *Closed chromatin loops at the ends of chromosomes.* J Cell Biol, 2004. **166**(2): p. 161-5.
37. Greider, C.W., *Telomeres do D-loop-T-loop.* Cell, 1999. **97**(4): p. 419-22.
38. Gilson, E. and V. Geli, *How telomeres are replicated.* Nat Rev Mol Cell Biol, 2007. **8**(10): p. 825-38.
39. Palm, W. and T. de Lange, *How shelterin protects mammalian telomeres.* Annu Rev Genet, 2008. **42**: p. 301-34.
40. Zhong, Z., et al., *A mammalian factor that binds telomeric TTAGGG repeats in vitro.* Mol Cell Biol, 1992. **12**(11): p. 4834-43.
41. Chong, L., et al., *A human telomeric protein.* Science, 1995. **270**(5242): p. 1663-7.
42. Bianchi, A., et al., *TRF1 is a dimer and bends telomeric DNA.* The EMBO journal, 1997. **16**(7): p. 1785-94.
43. Bilaud, T., et al., *Telomeric localization of TRF2, a novel human telobox protein.* Nat Genet, 1997. **17**(2): p. 236-9.
44. Broccoli, D., et al., *Human telomeres contain two distinct Myb-related proteins, TRF1 and TRF2.* Nat Genet, 1997. **17**(2): p. 231-5.
45. Ye, J.Z.S., et al., *TIN2 binds TRF1 and TRF2 simultaneously and stabilizes the TRF2 complex on telomeres.* Journal of Biological Chemistry, 2004. **279**(45): p. 47264-47271.
46. Liu, D., et al., *Telosome, a mammalian telomere-associated complex formed by multiple telomeric proteins.* Journal of Biological Chemistry, 2004. **279**(49): p. 51338-42.
47. Kim, S.H., P. Kaminker, and J. Campisi, *TIN2, a new regulator of telomere length in human cells.* Nat Genet, 1999. **23**(4): p. 405-12.
48. Chen, Y., et al., *A shared docking motif in TRF1 and TRF2 used for differential recruitment of telomeric proteins.* Science, 2008. **319**(5866): p. 1092-6.

49. O'Connor, M.S., et al., *A critical role for TPP1 and TIN2 interaction in high-order telomeric complex assembly.* Proc Natl Acad Sci U S A, 2006. **103**(32): p. 11874-9.
50. Ye, J.Z., et al., *POT1-interacting protein PIP1: a telomere length regulator that recruits POT1 to the TIN2/TRF1 complex.* Genes Dev, 2004. **18**(14): p. 1649-54.
51. Liu, D., et al., *PTOP interacts with POT1 and regulates its localization to telomeres.* Nat Cell Biol, 2004. **6**(7): p. 673-80.
52. Loayza, D. and T. De Lange, *POT1 as a terminal transducer of TRF1 telomere length control.* Nature, 2003. **423**(6943): p. 1013-8.
53. Li, B., S. Oestreich, and T. de Lange, *Identification of human Rap1: implications for telomere evolution.* Cell, 2000. **101**(5): p. 471-83.
54. Broccoli, D., et al., *Comparison of the human and mouse genes encoding the telomeric protein, TRF1: chromosomal localization, expression and conserved protein domains.* Human molecular genetics, 1997. **6**(1): p. 69-76.
55. Griffith, J., A. Bianchi, and T. de Lange, *TRF1 promotes parallel pairing of telomeric tracts in vitro.* Journal of molecular biology, 1998. **278**(1): p. 79-88.
56. Smith, S. and T. de Lange, *TRF1, a mammalian telomeric protein.* Trends in genetics : TIG, 1997. **13**(1): p. 21-6.
57. van Steensel, B. and T. de Lange, *Control of telomere length by the human telomeric protein TRF1.* Nature, 1997. **385**(6618): p. 740-3.
58. Karlseder, J., et al., *Targeted deletion reveals an essential function for the telomere length regulator Trf1.* Mol Cell Biol, 2003. **23**(18): p. 6533-41.
59. Fairall, L., et al., *Structure of the TRFH dimerization domain of the human telomeric proteins TRF1 and TRF2.* Mol Cell, 2001. **8**(2): p. 351-61.
60. Court, R., et al., *How the human telomeric proteins TRF1 and TRF2 recognize telomeric DNA: a view from high-resolution crystal structures.* EMBO Rep, 2005. **6**(1): p. 39-45.
61. Stansel, R.M., T. de Lange, and J.D. Griffith, *T-loop assembly in vitro involves binding of TRF2 near the 3' telomeric overhang.* EMBO J, 2001. **20**(19): p. 5532-40.
62. Smogorzewska, A., et al., *Control of human telomere length by TRF1 and TRF2.* Molecular and cellular biology, 2000. **20**(5): p. 1659-68.
63. van Steensel, B., A. Smogorzewska, and T. de Lange, *TRF2 protects human telomeres from end-to-end fusions.* Cell, 1998. **92**(3): p. 401-13.
64. Karlseder, J., et al., *p53- and ATM-dependent apoptosis induced by telomeres lacking TRF2.* Science, 1999. **283**(5406): p. 1321-5.
65. Shen, M., et al., *Characterization and cell cycle regulation of the related human telomeric proteins Pin2 and TRF1 suggest a role in mitosis.* Proc Natl Acad Sci U S A, 1997. **94**(25): p. 13618-23.
66. Zhu, Q., et al., *GNL3L stabilizes the TRF1 complex and promotes mitotic transition.* J Cell Biol, 2009. **185**(5): p. 827-39.
67. Nishiyama, A., et al., *Cell-cycle-dependent Xenopus TRF1 recruitment to telomere chromatin regulated by Polo-like kinase.* EMBO J, 2006. **25**(3): p. 575-84.
68. Mattern, K.A., et al., *Dynamics of protein binding to telomeres in living cells: implications for telomere structure and function.* Mol Cell Biol, 2004. **24**(12): p. 5587-94.
69. Meng, L., et al., *Nucleostemin inhibits TRF1 dimerization and shortens its dynamic association with the telomere.* J Cell Sci, 2011. **124**(Pt 21): p. 3706-14.
70. Ye, J.Z. and T. de Lange, *TIN2 is a tankyrase 1 PARP modulator in the TRF1 telomere length control complex.* Nat Genet, 2004. **36**(6): p. 618-23.
71. Smith, S., et al., *Tankyrase, a poly(ADP-ribose) polymerase at human telomeres.* Science, 1998. **282**(5393): p. 1484-7.

72. Wu, Y., S. Xiao, and X.D. Zhu, *MRE11-RAD50-NBS1 and ATM function as co-mediators of TRF1 in telomere length control.* Nat Struct Mol Biol, 2007. **14**(9): p. 832-40.
73. Lu, K.P. and X.Z. Zhou, *The prolyl isomerase PIN1: a pivotal new twist in phosphorylation signalling and disease.* Nat Rev Mol Cell Biol, 2007. **8**(11): p. 904-16.
74. Lee, T.H., et al., *Essential role of Pin1 in the regulation of TRF1 stability and telomere maintenance.* Nat Cell Biol, 2009. **11**(1): p. 97-105.
75. Chang, W., J.N. Dynek, and S. Smith, *TRF1 is degraded by ubiquitin-mediated proteolysis after release from telomeres.* Genes Dev, 2003. **17**(11): p. 1328-33.
76. Lee, T.H., et al., *The F-box protein FBX4 targets PIN2/TRF1 for ubiquitin-mediated degradation and regulates telomere maintenance.* J Biol Chem, 2006. **281**(2): p. 759-68.
77. Muramatsu, Y., et al., *Cross-species difference in telomeric function of tankyrase 1.* Cancer Sci, 2007. **98**(6): p. 850-7.
78. Dynek, J.N. and S. Smith, *Resolution of sister telomere association is required for progression through mitosis.* Science, 2004. **304**(5667): p. 97-100.
79. Ohki, R. and F. Ishikawa, *Telomere-bound TRF1 and TRF2 stall the replication fork at telomeric repeats.* Nucleic Acids Res, 2004. **32**(5): p. 1627-37.
80. Canudas, S., et al., *Protein requirements for sister telomere association in human cells.* The EMBO journal, 2007. **26**(23): p. 4867-78.
81. Cooper, J.P., Y. Watanabe, and P. Nurse, *Fission yeast Taz1 protein is required for meiotic telomere clustering and recombination.* Nature, 1998. **392**(6678): p. 828-31.
82. Chuang, T.C., et al., *The three-dimensional organization of telomeres in the nucleus of mammalian cells.* BMC biology, 2004. **2**: p. 12.
83. Gadji, M., et al., *Three-dimensional nuclear telomere architecture is associated with differential time to progression and overall survival in glioblastoma patients.* Neoplasia, 2010. **12**(2): p. 183-91.
84. Knecht, H., et al., *3D Telomere FISH defines LMP1-expressing Reed-Sternberg cells as end-stage cells with telomere-poor 'ghost' nuclei and very short telomeres.* Laboratory investigation; a journal of technical methods and pathology, 2010. **90**(4): p. 611-9.
85. Goldberg-Bittman, L., et al., *Telomere aggregates in non-Hodgkin lymphoma patients at different disease stages.* Cancer Genet Cytogenet, 2008. **184**(2): p. 105-8.
86. Kim, S.H., et al., *The human telomere-associated protein TIN2 stimulates interactions between telomeric DNA tracts in vitro.* EMBO reports, 2003. **4**(7): p. 685-91.
87. Azzalin, C.M. and J. Lingner, *Cell biology. Telomere wedding ends in divorce.* Science, 2004. **304**(5667): p. 60-2.
88. Zhu, L., et al., *Telomere length regulation in mice is linked to a novel chromosome locus.* Proc Natl Acad Sci U S A, 1998. **95**(15): p. 8648-53.
89. Barber, L.J., et al., *RTEL1 maintains genomic stability by suppressing homologous recombination.* Cell, 2008. **135**(2): p. 261-71.
90. Shete, S., et al., *Genome-wide association study identifies five susceptibility loci for glioma.* Nat Genet, 2009. **41**(8): p. 899-904.
91. Wrensch, M., et al., *Variants in the CDKN2B and RTEL1 regions are associated with high-grade glioma susceptibility.* Nat Genet, 2009. **41**(8): p. 905-8.
92. Egan, K.M., et al., *Cancer susceptibility variants and the risk of adult glioma in a US case-control study.* J Neurooncol, 2011. **104**(2): p. 535-42.
93. Sfeir, A., et al., *Mammalian telomeres resemble fragile sites and require TRF1 for efficient replication.* Cell, 2009. **138**(1): p. 90-103.
94. Miller, K.M., O. Rog, and J.P. Cooper, *Semi-conservative DNA replication through telomeres requires Taz1.* Nature, 2006. **440**(7085): p. 824-8.

95. Vannier, J.B., et al., *RTEL1 Dismantles T Loops and Counteracts Telomeric G4-DNA to Maintain Telomere Integrity.* Cell, 2012. **149**(4): p. 795-806.
96. Aubert, G., M. Hills, and P.M. Lansdorp, *Telomere length measurement-caveats and a critical assessment of the available technologies and tools.* Mutat Res, 2012. **730**(1-2): p. 59-67.
97. Shimomura, O., F.H. Johnson, and Y. Saiga, *Extraction, purification and properties of aequorin, a bioluminescent protein from the luminous hydromedusan, Aequorea.* J Cell Comp Physiol, 1962. **59**: p. 223-39.
98. Shaner, N.C., P.A. Steinbach, and R.Y. Tsien, *A guide to choosing fluorescent proteins.* Nat Methods, 2005. **2**(12): p. 905-9.
99. Conner, D.A., *Mouse embryonic stem (ES) cell culture.* Curr Protoc Mol Biol, 2001. **Chapter 23**: p. Unit 23 3.
100. Sineva, G.S. and V.A. Pospelov, *Inhibition of GSK3beta enhances both adhesive and signalling activities of beta-catenin in mouse embryonic stem cells.* Biol Cell, 2010. **102**(10): p. 549-60.
101. Matsuda, T., et al., *STAT3 activation is sufficient to maintain an undifferentiated state of mouse embryonic stem cells.* EMBO J, 1999. **18**(15): p. 4261-9.
102. Tichy, E.D., *Mechanisms maintaining genomic integrity in embryonic stem cells and induced pluripotent stem cells.* Exp Biol Med (Maywood), 2011. **236**(9): p. 987-96.
103. Cervantes, R.B., et al., *Embryonic stem cells and somatic cells differ in mutation frequency and type.* Proc Natl Acad Sci U S A, 2002. **99**(6): p. 3586-90.
104. Hong, Y., et al., *Protecting genomic integrity in somatic cells and embryonic stem cells.* Mutat Res, 2007. **614**(1-2): p. 48-55.
105. Aladjem, M.I., et al., *ES cells do not activate p53-dependent stress responses and undergo p53-independent apoptosis in response to DNA damage.* Curr Biol, 1998. **8**(3): p. 145-55.
106. White, J. and S. Dalton, *Cell cycle control of embryonic stem cells.* Stem Cell Rev, 2005. **1**(2): p. 131-8.
107. Griffin, C., et al., *The involvement of key DNA repair pathways in the formation of chromosome rearrangements in embryonic stem cells.* DNA Repair (Amst), 2005. **4**(9): p. 1019-27.
108. Jin, S., S. Inoue, and D.T. Weaver, *Differential etoposide sensitivity of cells deficient in the Ku and DNA-PKcs components of the DNA-dependent protein kinase.* Carcinogenesis, 1998. **19**(6): p. 965-71.
109. Gao, Y., et al., *A targeted DNA-PKcs-null mutation reveals DNA-PK-independent functions for KU in V(D)J recombination.* Immunity, 1998. **9**(3): p. 367-76.
110. Nagy, A., *Manipulating the mouse embryo : a laboratory manual*. 3rd ed2003, Cold Spring Harbor, N.Y.: Cold Spring Harbor Laboratory Press. viii, 764 p.
111. Levine, A.J. and M. Oren, *The first 30 years of p53: growing ever more complex.* Nat Rev Cancer, 2009. **9**(10): p. 749-58.
112. Sabapathy, K., et al., *Regulation of ES cell differentiation by functional and conformational modulation of p53.* EMBO J, 1997. **16**(20): p. 6217-29.
113. Hong, Y. and P.J. Stambrook, *Restoration of an absent G1 arrest and protection from apoptosis in embryonic stem cells after ionizing radiation.* Proc Natl Acad Sci U S A, 2004. **101**(40): p. 14443-8.
114. Liou, J.Y., B.S. Ko, and T.C. Chang, *An efficient transfection method for mouse embryonic stem cells.* Methods Mol Biol, 2010. **650**: p. 145-53.
115. Nagai, T., et al., *A variant of yellow fluorescent protein with fast and efficient maturation for cell-biological applications.* Nat Biotechnol, 2002. **20**(1): p. 87-90.
116. Geertsma, E.R., et al., *Quality control of overexpressed membrane proteins.* Proc Natl Acad Sci U S A, 2008. **105**(15): p. 5722-7.

117. Aoki, T., et al., *Construction of a fusion protein between protein A and green fluorescent protein and its application to western blotting.* FEBS Lett, 1996. **384**(2): p. 193-7.
118. Giraldez, T., T.E. Hughes, and F.J. Sigworth, *Generation of functional fluorescent BK channels by random insertion of GFP variants.* J Gen Physiol, 2005. **126**(5): p. 429-38.
119. Waldo, G.S., *Improving protein folding efficiency by directed evolution using the GFP folding reporter.* Methods Mol Biol, 2003. **230**: p. 343-59.
120. Rucker, E., et al., *Rapid evaluation and optimization of recombinant protein production using GFP tagging.* Protein Expr Purif, 2001. **21**(1): p. 220-3.
121. Kaba, S.A., et al., *Fusion to green fluorescent protein improves expression levels of Theileria parva sporozoite surface antigen p67 in insect cells.* Parasitology, 2002. **125**(Pt 6): p. 497-505.
122. Shaner, N.C., et al., *Improved monomeric red, orange and yellow fluorescent proteins derived from Discosoma sp. red fluorescent protein.* Nat Biotechnol, 2004. **22**(12): p. 1567-72.
123. Davoli, T., E.L. Denchi, and T. de Lange, *Persistent telomere damage induces bypass of mitosis and tetraploidy.* Cell, 2010. **141**(1): p. 81-93.
124. Ivankovic, M., et al., *Telomerase activity in HeLa cervical carcinoma cell line proliferation.* Biogerontology, 2007. **8**(2): p. 163-72.
125. Matlashewski, G., et al., *Analysis of human p53 proteins and mRNA levels in normal and transformed cells.* Eur J Biochem, 1986. **154**(3): p. 665-72.
126. Ohnuki, Y., *Structure of chromosomes. I. Morphological studies of the spiral structure of human somatic chromosomes.* Chromosoma, 1968. **25**(4): p. 402-28.
127. Onn, I., et al., *Sister chromatid cohesion: a simple concept with a complex reality.* Annu Rev Cell Dev Biol, 2008. **24**: p. 105-29.
128. Nasmyth, K. and C.H. Haering, *The structure and function of SMC and kleisin complexes.* Annu Rev Biochem, 2005. **74**: p. 595-648.
129. Uhlmann, F., et al., *Cleavage of cohesin by the CD clan protease separin triggers anaphase in yeast.* Cell, 2000. **103**(3): p. 375-86.
130. Pauli, A., et al., *Cell-type-specific TEV protease cleavage reveals cohesin functions in Drosophila neurons.* Dev Cell, 2008. **14**(2): p. 239-51.
131. Wehr, M.C., et al., *Monitoring regulated protein-protein interactions using split TEV.* Nat Methods, 2006. **3**(12): p. 985-93.
132. Kapust, R.B. and D.S. Waugh, *Controlled intracellular processing of fusion proteins by TEV protease.* Protein Expr Purif, 2000. **19**(2): p. 312-8.
133. Kurreck, J., *siRNA efficiency: structure or sequence-that is the question.* J Biomed Biotechnol, 2006. **2006**(4): p. 83757.
134. Banaszynski, L.A., et al., *A rapid, reversible, and tunable method to regulate protein function in living cells using synthetic small molecules.* Cell, 2006. **126**(5): p. 995-1004.
135. Rizzo, M.A., et al., *An improved cyan fluorescent protein variant useful for FRET.* Nat Biotechnol, 2004. **22**(4): p. 445-9.
136. Schultz, L.B., et al., *p53 binding protein 1 (53BP1) is an early participant in the cellular response to DNA double-strand breaks.* J Cell Biol, 2000. **151**(7): p. 1381-90.
137. Anderson, L., C. Henderson, and Y. Adachi, *Phosphorylation and rapid relocalization of 53BP1 to nuclear foci upon DNA damage.* Mol Cell Biol, 2001. **21**(5): p. 1719-29.
138. Houghtaling, S., et al., *Fancd2 functions in a double strand break repair pathway that is distinct from non-homologous end joining.* Hum Mol Genet, 2005. **14**(20): p. 3027-33.
139. Pryde, F., et al., *53BP1 exchanges slowly at the sites of DNA damage and appears to require RNA for its association with chromatin.* J Cell Sci, 2005. **118**(Pt 9): p. 2043-55.
140. Chan, K.L., et al., *Replication stress induces sister-chromatid bridging at fragile site loci in mitosis.* Nat Cell Biol, 2009. **11**(6): p. 753-60.

141. Vinciguerra, P., et al., *Cytokinesis failure occurs in Fanconi anemia pathway-deficient murine and human bone marrow hematopoietic cells.* J Clin Invest, 2010. **120**(11): p. 3834-42.
142. Gertsenstein, M., C. Lobe, and A. Nagy, *ES cell-mediated conditional transgenesis.* Methods Mol Biol, 2002. **185**: p. 285-307.
143. Lansdorp, P.M., et al., *Heterogeneity in telomere length of human chromosomes.* Hum Mol Genet, 1996. **5**(5): p. 685-91.
144. Oh, B.K., et al., *Up-regulation of telomere-binding proteins, TRF1, TRF2, and TIN2 is related to telomere shortening during human multistep hepatocarcinogenesis.* Am J Pathol, 2005. **166**(1): p. 73-80.
145. Matsutani, N., et al., *Expression of telomeric repeat binding factor 1 and 2 and TRF1-interacting nuclear protein 2 in human gastric carcinomas.* Int J Oncol, 2001. **19**(3): p. 507-12.
146. Yamada, K., et al., *Decreased gene expression for telomeric-repeat binding factors and TIN2 in malignant hematopoietic cells.* Anticancer Res, 2002. **22**(2B): p. 1315-20.
147. Yamada, M., et al., *Down-regulation of TRF1, TRF2 and TIN2 genes is important to maintain telomeric DNA for gastric cancers.* Anticancer Res, 2002. **22**(6A): p. 3303-7.
148. Miyachi, K., et al., *Correlation between telomerase activity and telomeric-repeat binding factors in gastric cancer.* J Exp Clin Cancer Res, 2002. **21**(2): p. 269-75.
149. Lin, X., et al., *Expression of telomere-associated genes as prognostic markers for overall survival in patients with non-small cell lung cancer.* Clin Cancer Res, 2006. **12**(19): p. 5720-5.
150. Soussi, T., et al., *Locus-specific mutation databases: pitfalls and good practice based on the p53 experience.* Nat Rev Cancer, 2006. **6**(1): p. 83-90.
151. Canudas, S. and S. Smith, *Differential regulation of telomere and centromere cohesion by the Scc3 homologues SA1 and SA2, respectively, in human cells.* J Cell Biol, 2009. **187**(2): p. 165-73.
152. Remeseiro, S., et al., *Cohesin-SA1 deficiency drives aneuploidy and tumourigenesis in mice due to impaired replication of telomeres.* EMBO J, 2012.
153. Nasmyth, K., J.M. Peters, and F. Uhlmann, *Splitting the chromosome: cutting the ties that bind sister chromatids.* Science, 2000. **288**(5470): p. 1379-85.
154. Hanaoka, S., A. Nagadoi, and Y. Nishimura, *Comparison between TRF2 and TRF1 of their telomeric DNA-bound structures and DNA-binding activities.* Protein Sci, 2005. **14**(1): p. 119-30.
155. Hsiao, S.J. and S. Smith, *Sister telomeres rendered dysfunctional by persistent cohesion are fused by NHEJ.* J Cell Biol, 2009. **184**(4): p. 515-26.